April 2024

Convergent Research
Roadmapping Workshop Report

Solid-State Far-UVC Emission

Jasper Götting
Vivian Belenky

Convergent Research
Biosecurity Team

Report on the Convergent Research

SOLID-STATE FAR-UVC EMISSION

Roadmapping Workshop held in June 2023

Cover image: Paul Green (Unsplash)
Report version 1.1 (2024-05-29)

On June 12 and 13, 2023, **Convergent Research** held a workshop on solid-state far-UVC emitters in New York, NY. Twenty-five scientists, industry experts, and representatives from philanthropic organizations gathered to review and discuss solid-state far-UVC development goals, approaches, and priorities. The workshop comprised four parts:

1. Discussions determining the **far-UVC device development goals**: target metrics on which emitter performance should be graded and sets of numerical milestones that emitters will eventually need to meet (**section 3**).

2. Discussions establishing and outlining the various material and design **approaches to solid-state far-UVC emission** (**section 4**).

3. A **forecasting exercise** to elicit a consensus on the timelines of the various emitter approaches, during which participants assigned date ranges to the performance milestones, generating a canonical view of the approaches' timelines (**section 5**).

4. **Concluding discussions and recommendations** based on the priorities, disagreements, and uncertainties elucidated by the forecasting exercise (**section 6**).

WORKSHOP PARTICIPANTS AND ACKNOWLEDGMENTS

The following people attended the workshop, contributed to the forecasts and discussions, and read and edited the final report:

Scott Burroughs, Uviquity
Seth Coe-Sullivan, NS Nanotech
Brent Fisher, Uviquity
Russel Kanjorsky, Uviquity
Michael Kneissl, Technical University of Berlin
Ioannis Kymissis, Columbia University
John L. Lyons, US Naval Research Laboratory
Neal Oza, Booz Allen Hamilton
Siddha Pimputkar, Lehigh University
Siddharth Rajan, The Ohio State University
Rick Rasansky, XCMR
Leo Schowalter, University of Central Florida, Lit Thinking, Nagoya University
Nathan Stoddard, Lehigh University
Nicolas Volet, UVLaser, UV Medico, Aarhus University
Songrui Zhao, McGill University

We thank them for their contributions.

We are also grateful to **Aleš Flídr**, **Tessa Alexanian**, **Juan Cambeiro**, and **Quinn Dougherty** for their help with setting up and running the workshop. Lastly, we thank **Jacob Swett**, **David Brenner**, **Ewan Eadie**, and **AJ Kourabi** for attending the event and contributing to the discussions.

Table of Contents

1. Executive summary

Far ultraviolet-C (far-UVC) is a promising emerging technology for air and surface disinfection as well as *in vivo* inactivation of multi-drug-resistant pathogens. Currently, the only widely available far-UVC emitters are krypton-chloride excimer lamps, which lack many desired performance characteristics and scale poorly in cost. In theory, the performance and scalability of solid-state sources, like LEDs, make them ideal for all lighting applications, but uncertainties around solid-state far-UVC emission remain.

To analyze the prospect for next-generation far-UVC sources, Convergent Research gathered representatives from academia, industry, and philanthropy to discuss development goals, approaches, and bottlenecks for solid-state far-UVC.

Aluminum gallium nitride (AlGaN) devices—primarily, but not exclusively, LEDs—and **second-harmonic generation (SHG) blue laser devices** were considered the most promising approaches and were regarded as having the greatest potential to achieve the relevant target metrics. A third viable approach, **cathodoluminescent devices**, was ultimately determined to be less promising and more analogous to excimer lamps than to LEDs: a transition technology that could perform well in the short and perhaps medium term but would ultimately not be competitive with either AlGaN or SHG devices. Based on these discussions, we recommend:

Research and development priorities: A universal priority across all approaches is in the development of far-UVC-transparent materials for p-side alloys, device encapsulants, filters, and other balance-of-system components. Another approach-agnostic priority is the development of aluminum nitride as a material platform. For any AlGaN-based approach—whether LEDs, laser diodes, or any other solid-state design—the priority is in understanding point defects, and in improving light extraction efficiency and doping. SHG device improvements—including refining blue laser diodes and their integration with nonlinear optical elements—lie along a different development path but are, in general, an R&D priority due to the greater uncertainty associated with their potential.

Funding strategies: While allocating resources to the identified R&D priorities is important, of potentially even greater importance is the funding of projects that will grow the far-UVC market and enable greater private investment into solid-state R&D. These projects include comprehensive safety studies, real-world effectiveness trials, infrastructure technology development, public outreach and education, and support for clear, comprehensive, and sensible standards for far-UVC air disinfection. Identifying potential beachhead markets and considering the role of advance market commitments and prizes can stimulate demand and further R&D investment.

2. Background

2.1. Motivation

The transmission of airborne diseases is an ongoing public health emergency. Prior to COVID-19, endemic respiratory infections incurred around $200 billion in economic costs and over $1 trillion in health costs in the US alone[1–4]; globally, over $100 trillion. In its acute phase, COVID-19 incurred a staggering $16 trillion in damages and over one million deaths in the US.[5,6] Though the acute phase of the pandemic is over[7,8], endemic COVID-19 will likely significantly increase the ongoing pre-pandemic costs. At the same time, the risk of future, potentially much more devastating pandemics is ever present and likely increasing.[9–11] Preventing the transmission of airborne pathogens indoors is a critical lever for reducing this toll and ongoing risk.

Disrupting the airborne route can be achieved by source control that prevents the release of infectious aerosols into the air (i.e., masks/respirators) or by increasing the number of equivalent air changes per hour (eACH) in the indoor space, which reduces the concentration of infectious aerosols. Increasing eACH can be achieved by natural ventilation (e.g., opening a window), increasing the central circulation rate of treated or fresh outside air, filtering the air (either in ducts or with portable air filters), and using germicidal ultraviolet light.

2.2. Germicidal ultraviolet light

Germicidal ultraviolet light (GUV), typically UV-C light with wavelengths of 200–280 nm (**Figure 1**), has been applied for water disinfection since the early 1900s and air and surface disinfection since the 1930s.[12,13] Because the primary wavelengths used for conventional GUV—commonly 254 nm and 265 nm—are actinic, air disinfection systems were typically installed in the upper room (UR-GUV). Active or passive air circulation then transports air to the upper room, where it is disinfected.

UR-GUV systems already have significant advantages over solely ventilation and filtration-based systems. They consume far less energy, produce no noise, take up no floor space, and can readily provide orders of magnitude more equivalent air changes per hour (eACH) at the same cost—between 24–100

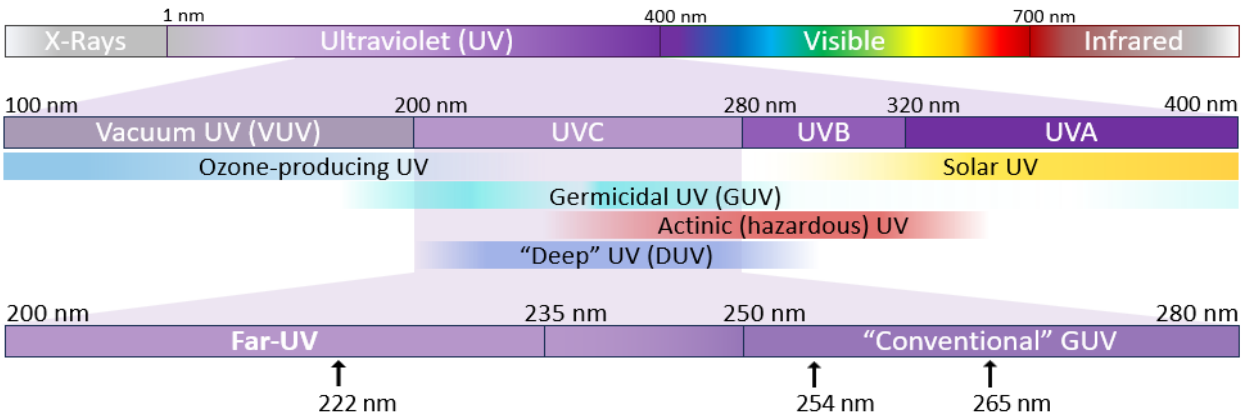

Figure 1: *The electromagnetic spectrum with annotated UV bands and common GUV wavelengths.*

eACH at ~$14/eACH—than can ventilation alone—up to 6 eACH at ~$135/eACH.* [14] Though neglected relative to its advantages, UR-GUV has limitations. Though very safe if used correctly[15], UR-GUV *must be used correctly*, incurring significant maintenance and verification costs—perhaps leading to public health officials' historical reluctance to recommend it out of safety concerns. Further, UR-GUV relies on air circulation and cannot disrupt short-range transmission. However, GUV is changing with the advent of far-UVC.

2.3. Far-ultraviolet C light

Far-ultraviolet C light (far-UVC or far-UV, 200–235 nm) is an emerging form of GUV with transformative implications. At a given dose, far-UVC—commonly at 222 nm—is about as effective at inactivating pathogens as conventional GUV (**Figure 2**)[16,17], but unlike conventional GUV wavelengths, far-UVC is heavily absorbed by proteins (**Figure 3a**), and mounting evidence suggests that rapidly germicidal doses of far-UVC pose no significant risk to human eyes and skin.[18] Properly filtered far-UVC has been demonstrated to not

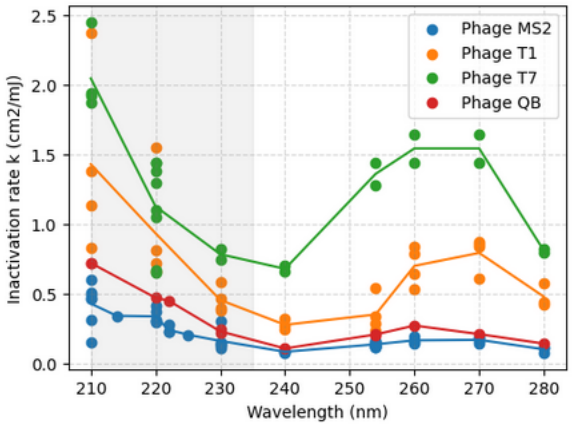

Figure 2: *Inactivation rates of common model organisms in solution. Data from Beck et al.*[16]

* It is more challenging to compare GUV to other technologies based on clean-air delivery rate (CADR), because GUV effectiveness roughly scales with room volume, while other technologies do not.

induce skin damage in humans, even up to very high doses[19], or in long-term exposed animals.[20]

Because of these safety properties, far-UVC can be deployed alongside ordinary light fixtures as "whole-room" systems. Not only is this approach safer and operationally simpler than UR-GUV, but it can potentially disrupt short-range or surface-based transmission of pathogens. It is also used for *in vivo* disinfection, e.g., against multi-drug-resistant pathogens in wounds. Promising settings for initial far-UVC installations are public locations with frequent airborne disease transmission: schools, airports, long-term care facilities, waiting rooms, and public transit. Agricultural applications, e.g., against crop pathogens or airborne livestock pathogens, and far-UVC-enhanced personal protective equipment are also possible.

2.4. Limitations of current emitters

Currently, the only commercially available light sources for far-UVC are krypton-chloride (KrCl) excimer lamps. KrCl excimer lamps have many desirable properties: they emit nearly monochromatically at 222 nm, can last up to 10,000 hours or longer, and have sufficient output power.

However, they have limitations. Though *nearly* monochromatic, KrCl excimer lamps require filtering to remove actinic wavelengths outside the far-UVC, which can be 10–20% of the total emission. Further, they can *only* produce 222 nm, and it is far from certain that 222 nm is the ideal far-UVC wavelength, as discussed further in **section 3.1.A**. Excimers require high voltages, which introduces design challenges to obtain energy efficiency and limit electromagnetic interference. Currently, they are highly energy inefficient with no identified path to increasing it significantly; commercial KrCl excimer lamps typically have wall-plug efficiencies of 1% or worse, resulting in a very high cost-per-watt.

The most important, however, is cost. Though KrCl excimer lamps are not currently produced at scale and are likely to fall from their current price point ($500–$2000 for fixtures using the market-leading Ushio B1 emitter) by perhaps up to an order of magnitude, their cost floor is likely to remain high (~$100). Their most natural analog is the fluorescent lamp, a transition technology. Much like how the white LED revolutionized the general lighting industry, solid-state far-UVC could revolutionize indoor biosafety.

3. Far-UVC device development goals

3.1. Ideal emitter performance

To be competitive with KrCl excimer lamps, a solid-state far-UVC source must deliver **better performance** at a **lower cost**.

Better performance for a far-UVC source is multifaceted. A performant far-UVC source will deliver the *correct intensity*, in *only the desired wavelengths*, *where it is needed*—for *as long as possible as cheaply as possible*.

All of these targets depend on uncertain inputs, and all of them influence the total cost of ownership the ultimate determining factor for the feasibility of adoption.

3.1.A Wavelength

To date, work has almost exclusively been done on 222 nm, the emission peak of KrCl excimer lamps.† In the next several years, 222 nm is likely to remain the dominant far-UV wavelength. However, there is no reason to believe that 222 nm is the *ideal* wavelength, and many reasons to consider shorter or longer ones:

- **Eye and skin safety**: Protein absorbance increases as wavelength shortens, such that more of the dose of a shorter wavelength will be fully absorbed in the upper layers of the stratum corneum of the skin and the mucin tear layer and corneal epithelium of the eye (**Figure 3a**).[18,26,27] Consequently, the American Conference of Governmental Industrial Hygienists (ACGIH) sets higher threshold limit values (TLVs®) for shorter far-UVC wavelengths (**Figure 3b**).[28] Using shorter wavelengths would enable a higher far-UVC dose to be delivered to occupied areas safely.

† Some data have recently become available for 233 nm.[21] Early data are also available for 207 nm produced by krypton-bromide excimer lamps[22,23], but krypton-bromide lamps have proved commercially intractable and have since largely been abandoned due to substantial efficiency, lifetime, and performance issues. Other wavelengths have been studied in laboratory settings using tunable lasers[24] and monochromators[25], but far from comprehensively.

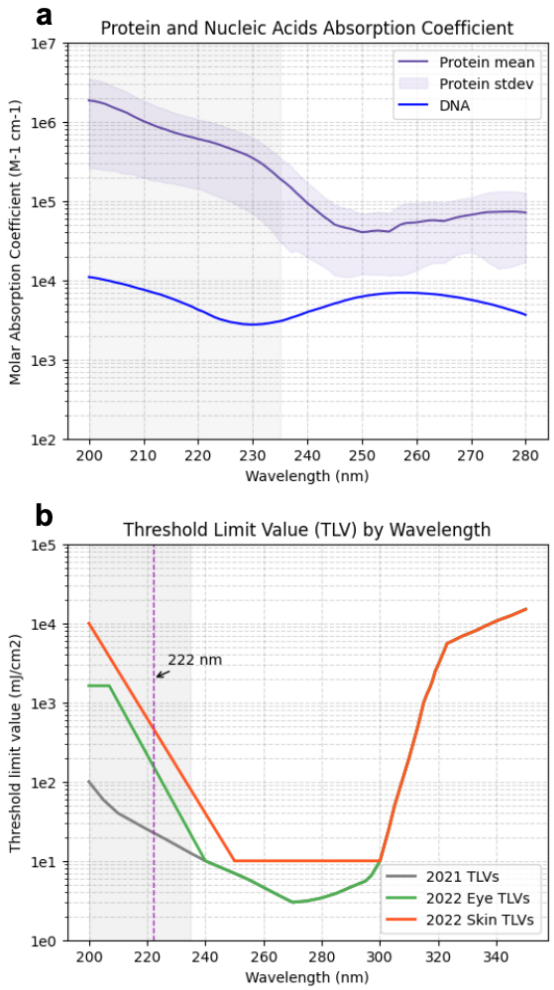

Figure 3: ***(a)*** *Protein and DNA absorbance by wavelength. Protein data derived from Kreusch.*[27] ***(b)*** *ACGIH-recommended threshold limit values (TLVs), old and new.*[28]

- **Ozone generation**: UVC wavelengths below 242 nm generate ozone by photocatalysis of oxygen in the air (Figure 4a). Ozone can then set off secondary reactions with volatile organic compounds (VOCs) usually present in indoor air, a process that eventually produces particulate matter (PM). While the absolute amount of ozone produced by far-UVC light under current TLVs is below occupational safety limits[29], the fact that the devices produce ozone in the first place and the ozone-induced secondary air chemistry might limit far-UVC deployment more strictly than photobiological safety alone.[30-33] The effectiveness of photocatalytic ozone generation rises as the wavelength shortens, favoring the longer end (225–235 nm) of the far-UVC spectrum for indoor use (Figure 4b). Ozone can be effectively managed with activated carbon or catalytic filters, so if vastly better disinfection could be safely achieved at the cost of a simple

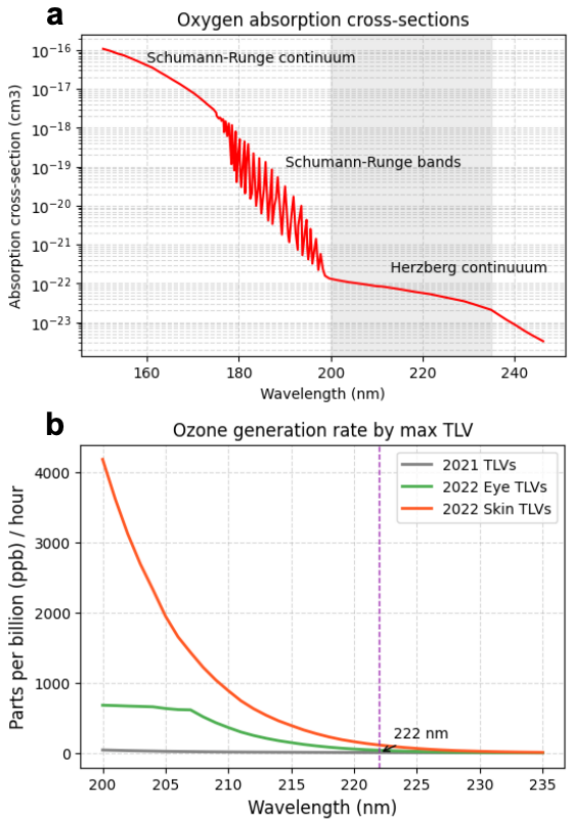

Figure 4: ***(a)*** *Oxygen absorption spectra. Increasing slowly over the far-UV, then rapidly in the vacuum UV.* ***(b)*** *Theoretical ozone generation by max TLV.*

catalytic ozone filter, then shorter wavelengths may still be preferable. However, there is ample reason to think this is not the case, mainly due to the effect of different wavelengths on efficacy.

- **Efficacy**: It is unclear what wavelength *best* inactivates pathogens, partly because the mechanism of inactivation by far-UVC wavelengths is not fully understood. Nominally, more protein absorbance at shorter wavelengths implies better efficacy—but respiratory pathogens are expelled in protein-rich saliva or airway mucus aerosols. Attenuation by the aerosols' significant protein content might make shorter wavelengths *less* effective at inactivation than longer wavelengths. Similarly, the inactivation of multi-drug resistant bacteria on human skin is weakened by far-UVC absorption in the protein-containing sweat layers and wound exudate. The mechanisms of far-UV interactions with protein and DNA may even be different across pathogen types (viruses, bacteria, fungi), in which case the ideal wavelength may vary by application.

Other considerations are even less well characterized, such as the wavelength-dependent degradation of plastics[34] or the effect on the skin microbiome.[35] Ultimately, which wavelength (or waveband) in the far-UVC gives the best reduction in airborne illness with the least hazard to human health is an open question (**Figure 5**).

Under these circumstances, at least some degree of **spectral tunability** is desirable. Production-level spectral tunability would allow manufacturers to target the optimal wavelength, roll out upgrades if new data emerge, and produce multi-wavelength or waveband systems on a single emitter platform. Emitters that are spectrally tunable during operation could even modulate their output wavelengths and optimize disinfection performance depending

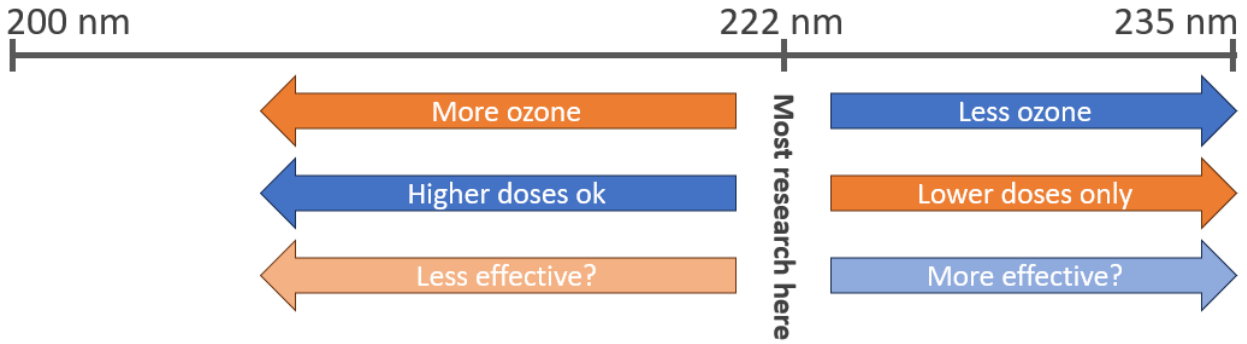

Figure 5: *Possible trade-offs of different far-UVC wavelengths. Effectiveness by wavelength strongly depends on the degree of attenuation by proteins in aerosols.*

on parameters like pathogen presence and type, room occupancy, or ozone concentration.

3.1.B Minimizing unwanted wavelengths

While the ability to target the right wavelength is important, it is equally important to exclude undesired wavelengths. A good far-UVC source should be confined to the far-UVC, i.e., it should not emit actinic UV (235–315 nm) or heavily ozone-producing vacuum UV (100–200 nm).

The presence of unwanted wavelengths limits the effective output power of a far-UVC source since non-far-UVC wavelengths bring the system closer to exceeding occupational exposure limits. In the case of actinic wavelengths, this is especially important as each part of a UV source's spectrum contributes to the exposure limit. As a result, though adding a filter to a KrCl far-UVC lamp reduces the 222 nm emission peak, it increases the *effective* available disinfection power manyfold by allowing a much longer exposure time before reaching the TLVs (**Figure 6**).

Though effective, filtering adds costs, lowers total output, and limits flexibility. There are no commercially available absorptive filters that work in far-UVC, and interference filters are only available for wavelengths above ~220 nm. Interference filters also exhibit angle-dependent performance, with unwanted wavelengths tending to "leak" heavily at extreme angles.

For this reason, a truly ideal far-UVC source would be tunable and **monochromatic**—it should emit the

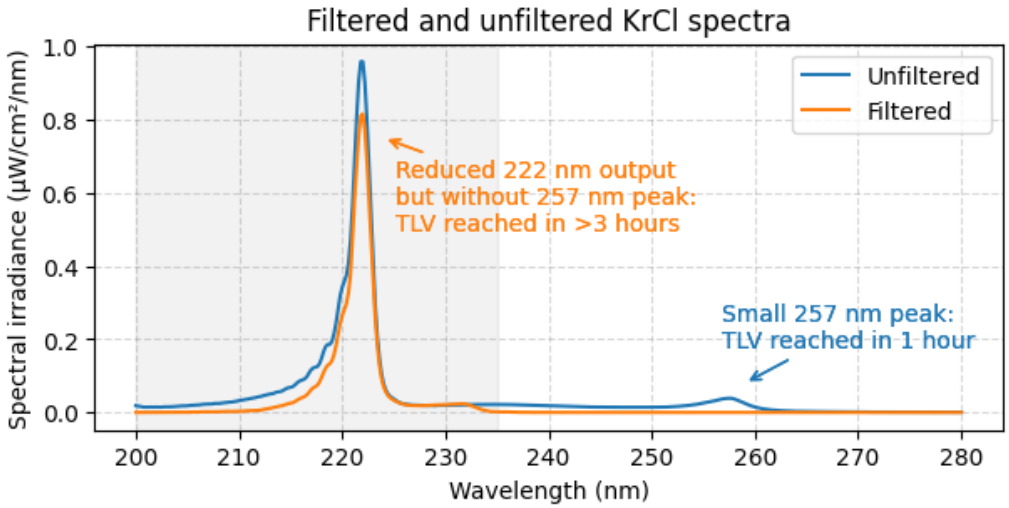

Figure 6: *Filtered and unfiltered spectra of a krypton-chloride excimer lamp.*

desired far-UVC wavelength, and *only* that wavelength.

3.1.C Power output

Ideal power output is uncertain for the same reason ideal wavelength is uncertain: the true tradeoffs between infection reduction and the downsides of far-UVC—like eye and skin irritation, potential material degradation, or ozone generation—are not well understood or vary by application.

Further, pathogens vary in their susceptibility to germicidal UV by their inactivation constant *k*. Under the same conditions, a UV-sensitive pathogen can be inactivated an order of magnitude faster than a UV-resistant pathogen. Pathogens also vary in their transmissibility. For two equally UV-sensitive pathogens, relatively low levels of UV intensity may be enough to prevent an outbreak of one but not the other.

For example, in an ordinary SARS-CoV-2 transmission scenario[36], even a fluence rate of 1 μW/cm² in an idealized classroom would be sufficient to drive the risk of infection below 1%. However,

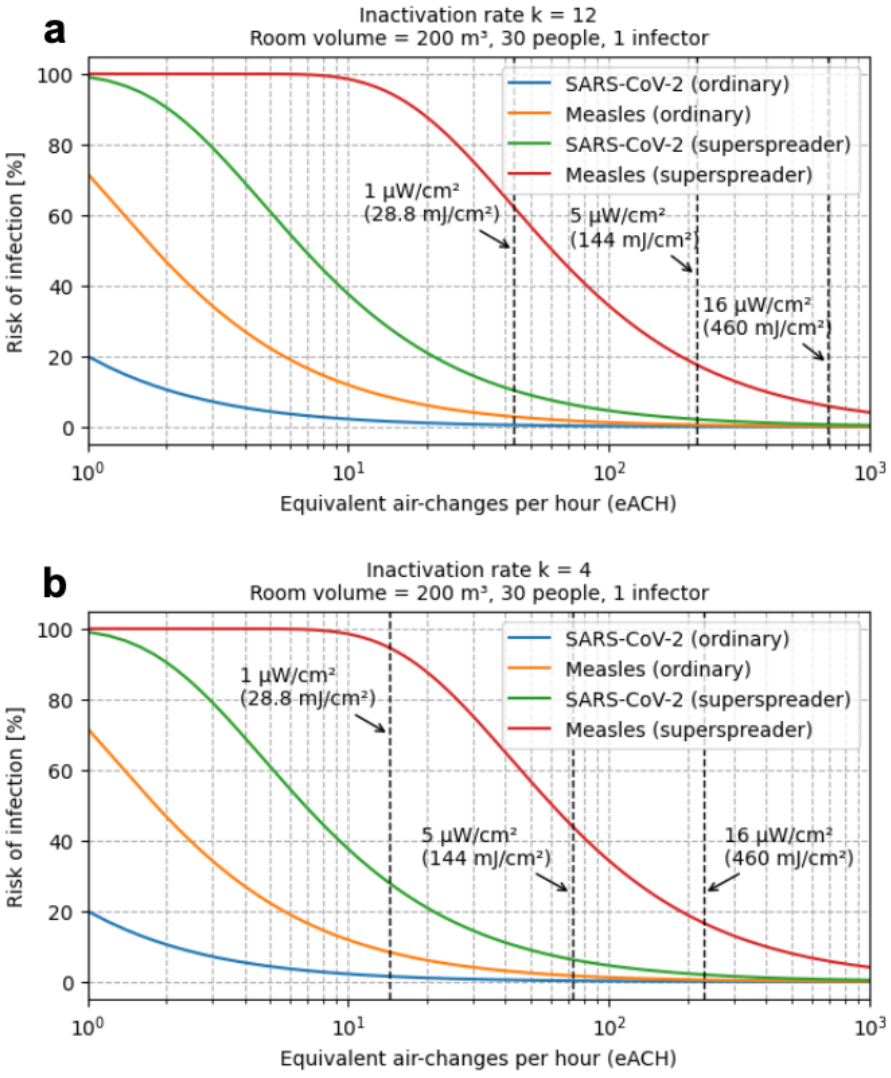

Figure 7: *Risk of infection by level of far-UVC irradiance, assuming* ***(a)*** *an inactivation rate* k *of 12 or* ***(b)*** *an inactivation rate* k *of 4.*

an ordinary measles transmission scenario requires at least 5 μW/cm^2 for a <1% infection risk. Importantly, neither the measles nor SARS-CoV-2 superspreader event is pushed to below 1% infection risk by 16 μW/cm^2, the maximum irradiance level permissible by the 2022 ACGIH skin TLVs—assuming that the light was distributed perfectly evenly in the space (**Figure 7a**). As superspreaders are often the main drivers of epidemics and pandemics, these scenarios are not just hypothetical worst cases but the central transmission events that air disinfection systems need to be able to prevent.[37,38]

If *k* is substantially lower, for example, via serious attenuation by respiratory aerosols, the case for higher power is even stronger (**Figure 7b**).

These estimates are intentionally designed to be closer to a "worst-case," but they demonstrate reasonable edge cases where high output power may be desirable.

For these reasons, it is ideal to have a source with a degree of **operational flexibility**. It should *(a)* be **dimmable**—capable of delivering the exact desired power output without significant loss of efficiency or shortening of lifetime—and *(b)* have a **high margin**—capable of increasing the output manyfold in epidemic scenarios with highly infectious, UV-resistant pathogens, where photobiological safety and ozone concerns are secondary. **Pulsed operation** may also be desirable as it might provide higher disinfection effectiveness at lower doses.[39–41]

3.1.D Form factor

There are several reasons to prefer a flexible, chip-based form factor for a light emitter over a bulky single lamp. The first is light uniformity.

In addition to the spectral properties of the light source, light uniformity is critical for building optimal disinfection systems. In most applications, maximum efficacy requires the **average fluence rate** to be as high as possible, whereas exposure safety is limited by the **maximum irradiance** at any point. This means that ideal systems will have a high degree of light uniformity–where the average fluence rate and maximum irradiance are close together.

To illustrate, in **Figure 8**, both rooms (seen in plan-view from above) have comparable average fluences around 1 μW/cm^2. However, room 1 quickly exceeds the eye TLVs while room 2

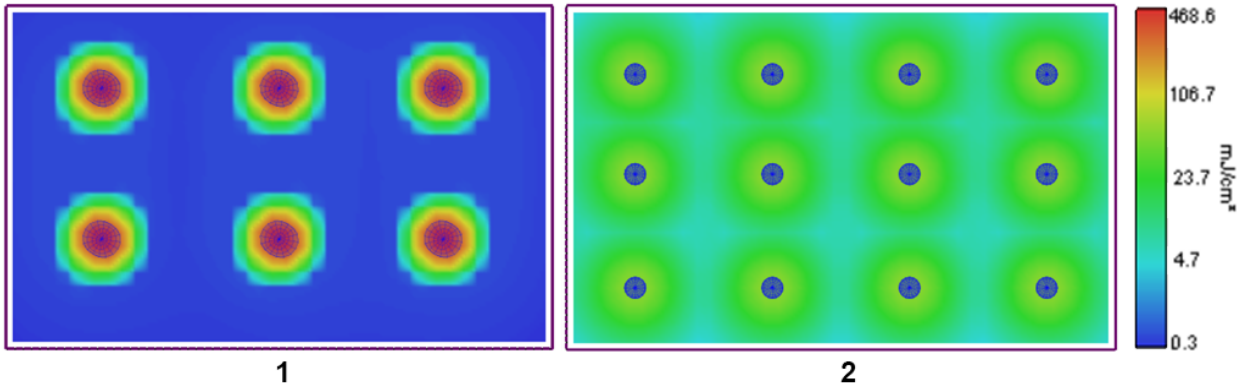

Figure 8: *Spatial distribution of the maximum dose over eight hours at a height of seven feet in two identical rooms with comparable average fluences. Room 1 contains six lamps generating far-UVC hotspots; room 2 contains twelve lamps with a more diffuse emission.*

stays comfortably within them. The improved uniformity not only reduces photobiological risk but also improves efficacy by reducing the system's reliance on moving air.

A smaller form factor allows for significant design flexibility—light packages can be distributed into many smaller fixtures in a variety of arrangements that would allow a designer more options to achieve good, safe system performance. This is especially important when ceiling height, existing fixtures, and room arrangement may all play a factor in what disinfection levels may be safely achieved. Another element of design flexibility that is only possible in a small form factor is the increased ability to shape the emission cone as early and efficiently as possible, e.g., by employing ultra-reflective packaging materials or refractive optics. In theory, low-cost far-UVC lasers would allow for the most flexible, targeted light delivery, as the emission can be directed, diffracted, or diffused relatively easily into beams, light sheets, more complex patterns, or uniform emission; ideal for delivering high (above-TLV) intensities to unoccupied spaces, e.g., between occupants at a meeting desk.

The final major reason to prefer a flexible form factor is simple aesthetics. Architects, designers, and building owners care about how a space looks and may pass on a more effective system if it is ugly or even just aesthetically mismatched. Flexible form factors for light emitters allow for the use of a wider variety of luminaires in a wider variety of styles and enable systems that both work well and look good.

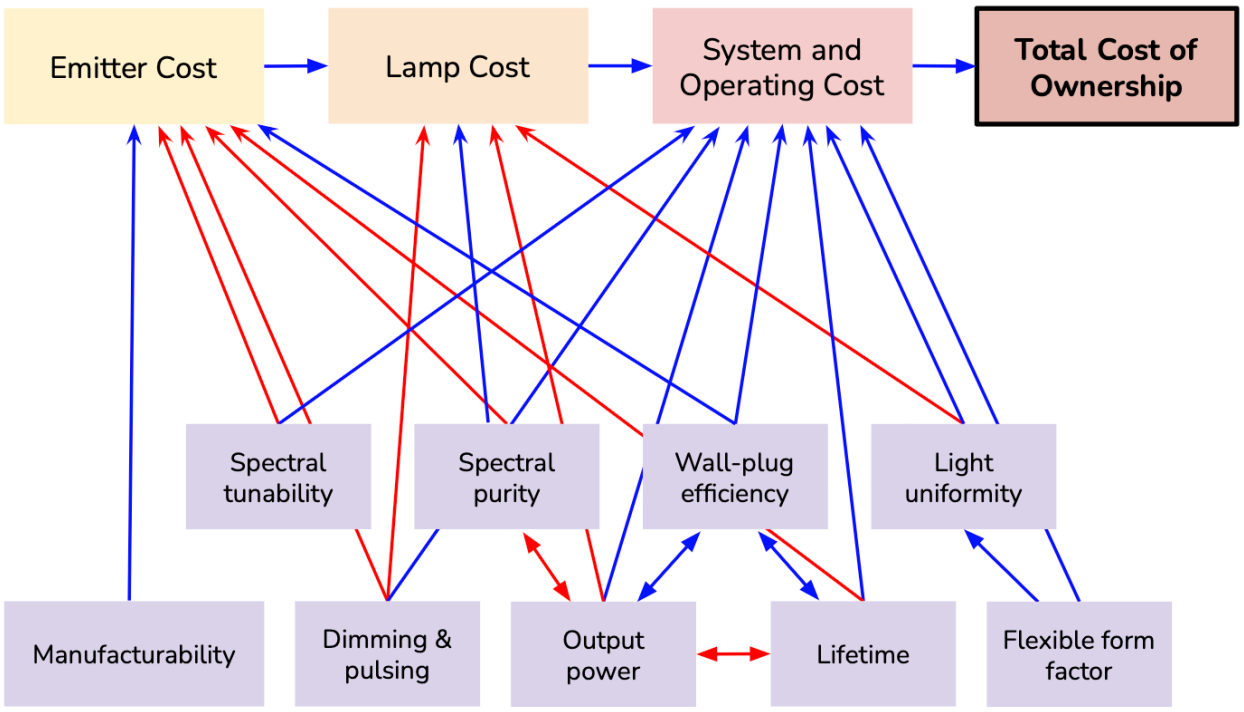

Figure 9: *Factors determining the total cost of ownership of a far-UVC air disinfection system. Blue lines indicate a positive influence between factors, and red lines represent a trade-off.*

3.2. Cost

Cost is another relatively ambiguous proposition, especially in a nascent market, but it will ultimately be one of the most important factors determining far-UVC uptake. It is often useful to operationalize cost in terms of **total cost of ownership (TCO)**, e.g., dollar per watt of far-UVC output, amortized over a 10-year period of 8-hour operation. TCO encompasses all the costs required to achieve the desired amount of air disinfection (Figure 9).

Acquisition costs encompass the cost of a light source, the number of light sources required, as well as the labor required to install them. Buyers are most likely to be sensitive to this cost, and it may have an outsized impact on enabling widespread adoption. The remaining costs are largely in number of replacements required (as well as the labor to make those replacements), as well as some minor contribution from cost of electricity.

However, it is difficult to operationalize these quantities directly when setting goals for emitter development. Instead, we operationalize along several factors that affect the TCO at different levels—though these effects are not always obvious or straightforward

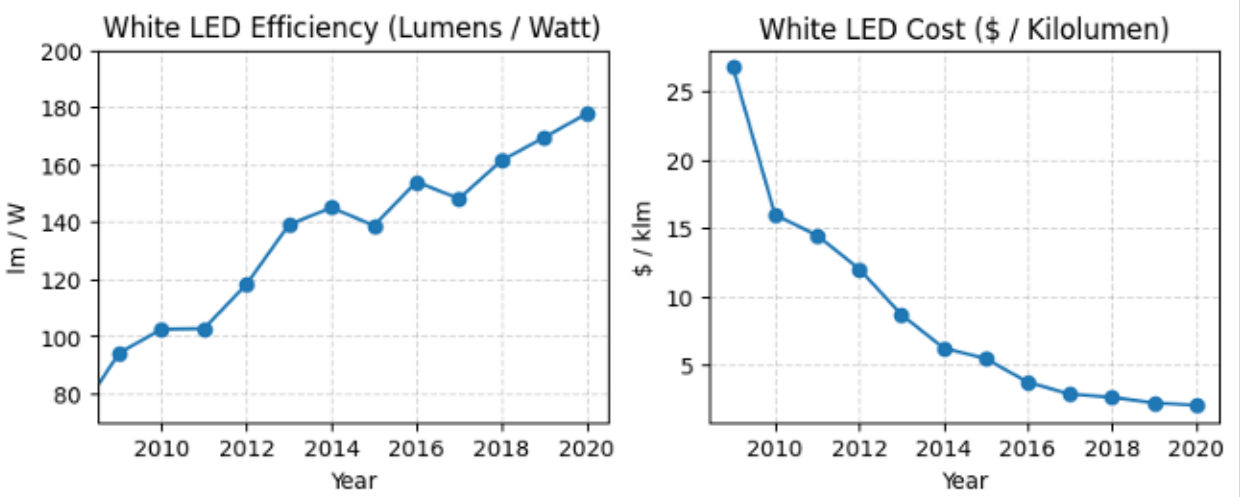

Figure 10: *Average white LED efficiency and cost over time. Efficiency tracks costs, though imperfectly.*[43]

3.2.A Emitter and lamp cost

We break down the costs of a light source into **emitter cost** and **lamp cost**. The emitter itself is the discharge bulb, cathode ray tube, LED chip, etc. The lamp includes the emitter, but also driving electronics, and potentially a filter, diffuser, or reflector. (We do not directly consider the cost of a luminaire, the final housing for the lamp.)

The emitter cost can be directly operationalized as the cost in USD per mW of far-UVC output and is influenced by several factors, the most important ones being:

Efficiency: Department of Energy reports on LEDs have historically focused on wall-plug efficiency (WPE) as a proxy for cost (**Figure 10**).[42,43] Increased efficiency usually allows for easier optimization of other parameters, but efficiency is not necessarily everything. A source might be highly efficient but still require significant upfront investment, a complicated manufacturing process, or more expensive materials.

Closely linked to WPE is **output power**. In solid-state emitters, like LEDs, both factors together determine the device size (and thus wafer yield) required to meet device specifications. Aside from its connection to WPE, output power is also an important target in itself, as effective disinfection requires a certain dose (see **section 3.1.C**). Importantly, output power trades off negatively with lifetime in LEDs. Running the device at higher currents degrades the materials and introduces defects that continuously reduce output and increase the probability of sudden failures, increasing operating costs.

Manufacturability: The ability to capitalize on economies of scale is the dominant determinant of a technology's likelihood of becoming cheap enough to be ubiquitous. Chip-based emitters profit from the highly scalable semiconductor fabrication infrastructure that can achieve extremely low production costs at scale. On the other hand, complex packaging techniques and exotic far-UVC-compatible materials can increase the device production cost again, not just for semiconductor emitters but for any far-UVC device that requires filtering. Some technologies can be relatively cheap even at small scales, even if other technologies would scale much better. As mentioned, the wafer yield of solid-state emitters can be further increased by making the devices more efficient and powerful, and thus smaller and ultimately cheaper.

3.2.B System and operating cost

The **system and operating cost** is influenced by the lamp cost, as well as lamp reliability, lifetime, and electrical efficiency.

Even with individually cheap lamps, uptake might be low if the TCO is dominated by large system and operating costs. To keep these costs low as well, the emitters must be primarily long-lasting but also versatile and effective.

Lifetime and reliability: Reliably long emitter lifetimes are important for convenient and inexpensive operation. Short lifetimes and the resulting frequent bulb or device replacements can drastically increase the system's TCO, especially if maintenance is labor-intensive. Even if direct replacement costs are low, system owners may simply forgo maintenance if it is too frequently required—as with filters for portable air cleaners, for example. Emitters should reliably operate for at least 10,000 hours (~2 years of 12 hours/day operation) without degrading below a specified performance threshold that ensures sufficient disinfection effectiveness (e.g., the L70 value—the time after which an LED has dropped to 70% of its initial output—as measured by a UV-adapted version of the IES LM-80 standard).

Versatility and effectiveness: To keep system costs down, emitters should be usable in a wide variety of applications and environments, having a flexible form factor that readily allows the design of any desired emission field to make system design and installation straightforward, universal, and cheap.

System cost also decreases the more effective the individual emitters are. As outlined in **section 3.1.**, this requires sufficient output power, an optimal emission spectrum, and uniform light delivery; all factors that increase the cost of individual emitters and lamps but ultimately result in cheaper systems.

3.3. Milestones

In summary, the ideal far-UVC emitter is:

1. Cheap
2. Efficient
3. Long-lasting
4. Dimmable
5. Monochromatic
6. Flexible (at least somewhat) in wavelength

To forecast future far-UVC emitter performance and evaluate different emitter approaches, we selected the three most important target metrics:

Emitter cost in USD per milliwatt, device efficiency (WPE) in percent, and lifetime in hours. For those targets, we selected three phases of performance milestones (**Table 1**).

Phase 1: The near term

These milestones are either already met or will be met within the next year by both KrCl excimer lamps as well as solid-state sources, i.e., far-UVC LEDs. KrCl excimer lamps currently cost 5–10 $/mW, achieve a WPE of ~1%, a lifetime of 10,000 hours, and have negligible emission above 235 nm when properly filtered. Any emitter meeting the phase 1 milestones can be used for research and niche applications but is not performant and cheap enough for widespread use and commercialization. To put the current performance into perspective: at $10/mW and a lifetime of 10,000 hours, it would cost about $11,000 per year in emitters alone to equip an average classroom with far-UVC.[‡]

Phase 2: The achievable

The Phase 2 milestones can likely be achieved by a far-UVC emitter within the next five years. Cost and WPE milestones are within reach of next-generation KrCl excimer lamps, and lifetime and non-far-UVC emission milestones are already met. With a cost of $1/mW

[‡] Eye TLVs are ~150 mJ/cm² over 8 hours, which equals an intensity of 50 mW/m². A typical classroom of 65 m² size thus requires 3.25 W of far-UVC. Lamps last about 3 years when operated 8 hours per day.

and a lifetime of 10,000 hours, the costs of emitters for equipping a classroom would decrease by an order of magnitude to just $1100.

Phase 3: The ideal high-performance

The Phase 3 milestones represent an ideal future far-UVC emitter. A lifetime of 25,000 hours is plausibly achievable by improved KrCl excimer lamp designs. A cost of $0.10/mW and a WPE of 10%, however, will likely only be attainable by solid-state sources. Equipping the typical classroom with a far-UVC emitter costing $0.10/mW and lasting 25,000 hours would only amount to $45 in emitters per year, almost 250-fold cheaper than currently possible.

In the following section, we discuss possible pathways to the achievement of these milestones.

Table 1: *The target metrics and their associated performance milestones.*

		Target metrics		
		Cost ($/mW)	*WPE (%)*	*Lifetime (h)*
Phase 1 milestones	*Milestones likely to be reached in the near term*	10	1	1,000
Phase 2 milestones	*Milestones that are achievable*	1	3	10,000
Phase 3 milestones	*Milestones for an ideal high-performance device that could eventually be met*	0.10	10	25,000

4. Approaches to solid-state far-UVC emission

4.1. Aluminum gallium nitride devices

4.1.A Background

AlGaN, the current UVC LED material platform, was developed from the highly successful gallium nitride (GaN) platform for blue LEDs. Work on the characterization, growth, and doping of GaN in the 1980s and '90s (awarded the Nobel prize in physics in 2014) paved the way for the modern high-efficiency (~60–80%) indium gallium nitride (InGaN) 450 nm blue LEDs.[44-48]

Substituting aluminum for indium increases the band gap deep into the UV region, allowing emission between 210 to 365 nm, depending on the relative proportion of aluminum to gallium. The InGaN platform is backed by a substantial industry around blue LEDs for solid-state lighting and displays, and UVA LEDs for curing applications.

AlGaN UV LEDs have benefited from many InGaN LED insights, and the efficiency of UVC LEDs in the 250–280 nm spectral band has been steadily improving, mirroring the development curve seen in blue LEDs and closing in on 10% WPE. However, the development of efficient far-UVC LEDs has proven to be particularly challenging.[49]

Box 1: Determinants of LED efficiency

The overall performance of an LED's electron-to-photon conversion is expressed as the **wall-plug efficiency (WPE)**, which is typically between 40 and 80% for LEDs emitting in the visible spectrum. WPE is the ratio between output power and input power (operating current times operating voltage). This ratio is determined by the **external quantum efficiency (EQE)** and the electrical or **voltage efficiency (η_{el}):**

$$WPE = \frac{P_{out}}{I \cdot U} = EQE \cdot \eta_{el}$$

EQE is determined by the **internal quantum efficiency (IQE)** and the **light extraction efficiency η_{ext}**—the ratio of photons leaving the LED chip to photons being generated inside the LED chip.

$$EQE = IQE \cdot \eta_{ext}$$

The IQE comprises the **radiative recombination efficiency η_{rad}** and **carrier injection efficiency η_{inj}**, two closely related parameters that describe the efficiency of injecting electron–hole pairs into the LED and recombining them to produce photons:

$$IQE = \eta_{rad} \cdot \eta_{inj}$$

Thus, WPE is determined by four efficiencies:

$$WPE = \eta_{rad} \cdot \eta_{inj} \cdot \eta_{ext} \cdot \eta_{el}$$

While WPE is ultimately the value that will determine the cost per watt of an LED, EQE is the most relevant value for most research applications.

4.1.B Challenges and prospects

Most challenges arise as the aluminum content of AlGaN is increased to shorten the emission wavelength. While lower-Al 280 nm UVC LEDs achieve up to 20% EQE (and 5-10% WPE), efficiencies below 250 nm and into the far-UVC (<235 nm) decrease by an order of magnitude (**Figure 11**), with LEDs in the longer-wavelength far-UVC (230–235 nm) just now reaching 1–2% WPE.[50–52]

The low WPE of far-UVC LEDs is multifactorial; low carrier injection efficiency, radiative recombination efficiency, light extraction efficiency, and electrical efficiency combine into an even lower WPE. Research has identified major challenges for reaching high efficiencies in increasingly aluminum-rich AlGaN far-UVC LEDs (**Table 2**).

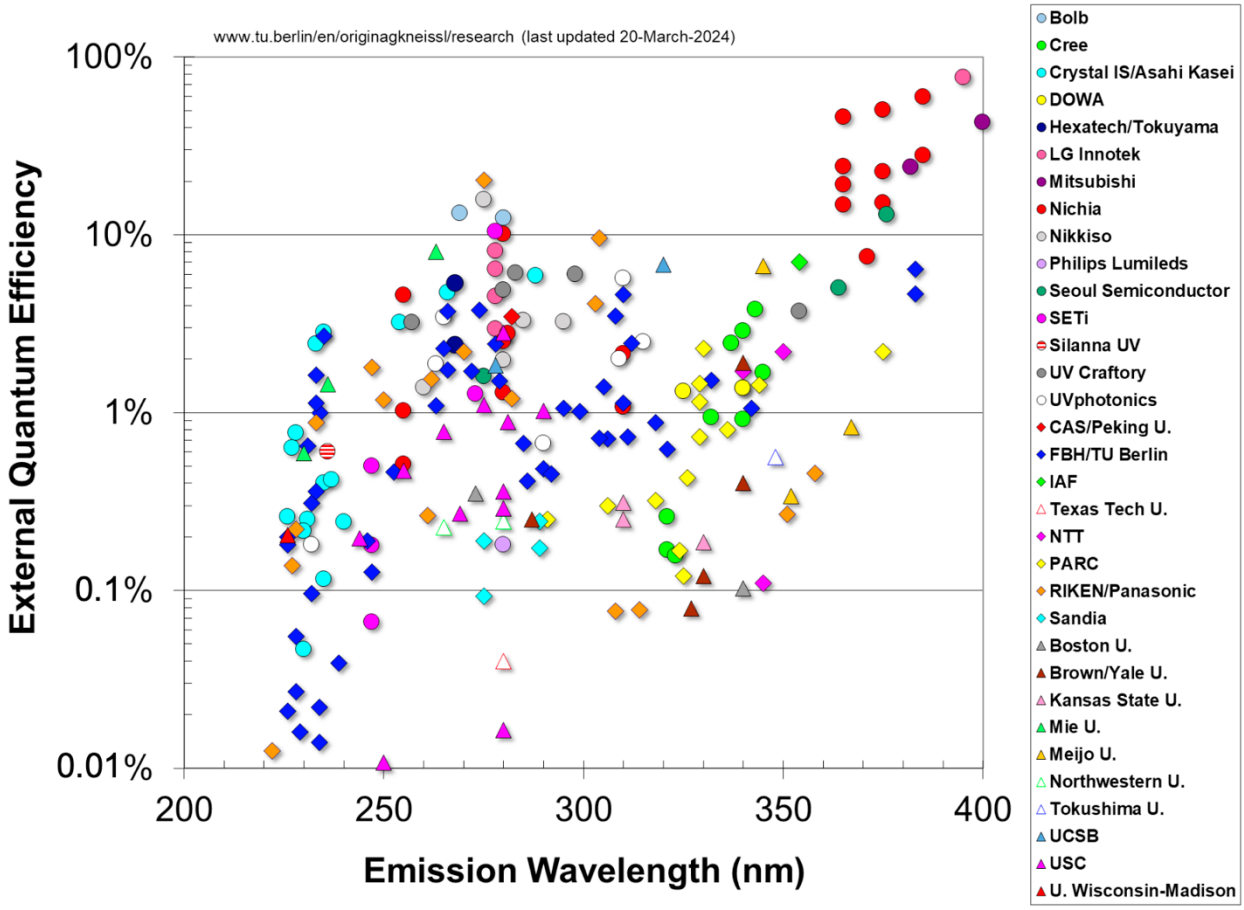

Figure 11: *External quantum efficiencies (EQE) of UV LEDs (2024) by Michael Kneissl.*[52]

Table 2: *Limitations of UV LED efficiencies. Efficiencies are based on a ~1% EQE 233 nm far-UVC LED described in Kolbe et al., 2023, and were estimated by the authors.[53] The efficiencies are higher for conventional UVC LEDs, but the ranking of the limitations—light extraction efficiency being the lowest and electrical efficiency being the highest—remains similar.[49]*

Factor	Limitation	Possible solutions
η_{ext} ~10%	P-doped GaN (used in the top contact layer) is opaque to far-UVC and reabsorbs some of the generated photons.[54]	Thin-film flip devices with reflective contact layers (e.g., p-Si, Ni/Ag, Mg/Al).[55–57] Transparent conducting oxide contact layers.[58,59] Tunnel-junction LEDs with UV-transparent n-AlGaN.[60]
	High-Al AlGaN favors TM emission (perpendicular to the plane of the device) instead of TE emission (orthogonal to the plane of the device).[54]	Device packaging and structuring that redirects side-emitted light upward.[61] SPSL LEDs.[62] Micro-LEDs.[63]
	Total reflection at multiple layer boundaries prevents the emission of generated photons.[54]	Micro- or nanophotonic structures on the device's emission face.[64,65]
η_{inj} ~25%	Inefficient hole injection as high-Al AlGaN is difficult to p-dope with magnesium.[54]	Alternative doping approaches, such as polarization doping.[53,66] Different materials as hole injection layers (e.g., h-BN, p-Si).[55,67]

	Electron leakage through the electron-blocking layers (EBL) surrounding the intrinsic layer.[49]	Alternative EBL designs, such as multiple quantum barrier EBLs.[68]
η_{rad} ~45%	Point defects in the active region trigger non-radiative recombinations.[54] Growing defect-free AlGaN epilayers of the highest possible quality also becomes increasingly difficult, as higher aluminum concentrations require higher temperatures.	Improved growth methods. Using native AlN substrate instead of sapphire with annealed AlN buffer layers.
	The quantum-confined Stark effect (QCSE) reduces the probability of radiative recombination.[54]	Novel intrinsic layer designs using band engineering, nonpolar AlGaN, or ultrathin MQWs.[54,69]
	At high current densities, the increasing prevalence of Auger–Meitner recombination leads to an efficiency droop.[70,71]	Increase active region volume. Balance electron–hole injection.[72] Improve electron-blocking.[73]
η_{el} ~65%	The high spreading resistance of high-Al n-AlGaN necessitates a high driving voltage.	Graded heterostructures.
	Non-ohmic electrical contacts to high-Al n-AlGaN result in higher operating voltages.	Novel metallization schemes and surface treatments.[74]

Light extraction is the largest efficiency loss in far-UVC LEDs, followed by low internal quantum efficiency and mediocre electrical efficiency. Importantly, the efficiency factors interact with and determine the device's lifetime. In LEDs, lifetime is mainly determined by drive current, temperature, and defect density.[75] At high currents and high temperatures, stress-induced degradation, exacerbated by existing crystal defects, can decrease lifetimes dramatically. To reduce the temperature and current densities and increase the lifetime of low-WPE far-UVC LEDs, devices are driven at low currents, limiting far-UVC output. Lifetime thus limits low-efficiency emitters, and low efficiencies limit lifetime. Addressing the efficiency bottlenecks and improving WPE is thus key to achieving lifetime development goals.

Fortunately, the long research history and large scientific community around the AlGaN material platform have produced different promising approaches and designs to mitigate those losses.

4.1.C Device types

Most far-UVC LEDs follow the traditional *p–i–n* LED design of an intrinsic layer,

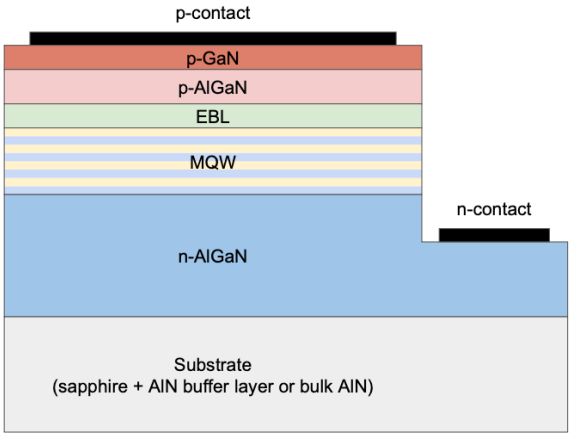

Figure 12: *A typical AlGaN LED stack.*

usually an AlGaN multi-quantum well (MQW) structure, sandwiched between p-type and n-type doped AlGaN, epitaxially grown on a substrate (**Figure 12**). Already, the first important distinction concerns devices grown on native (AlN) versus non-native (sapphire) substrates.

Substrate choice

To date, most AlGaN devices are grown on sapphire due to the material's low cost and good UV transparency, as well as large wafer size (up to 8 inches). However, there is a large lattice mismatch between sapphire and AlN, resulting in the generation of a large number of threading dislocations (i.e., line defects) at the AlN/sapphire interface. Various template technologies have been developed to reduce the defect densities in the AlN/sapphire. Typically, a thin AlN buffer layer is sputtered on the sapphire

wafer and annealed at very high temperatures (~1700°C), serving as the template on which the device is epitaxially grown. In contrast, a native AlN substrate allows for direct epitaxial growth and, subsequently, lower threading dislocation densities (TDD).

The development of AlN substrates has improved to the point that 2" wafers are commonly available, and 4"–6" wafers are expected to reach the market in the coming years. However, annealed sapphire wafers are still orders of magnitude cheaper than native AlN wafers, so cost reductions in bulk AlN growth will be necessary to make them cost-competitive.

Flip chip devices

The opaque p-side of traditional AlGaN UVC LEDs necessitates alternative device architectures. UVC LEDs usually follow a bulk flip chip or thin film flip chip design, in which the LED is flipped and bonded on its p-side to a submount wafer, either with the full thickness of the substrate (bulk flip chip) or with the substrate removed (thin film flip chip) down to a thin AlN buffer layer.[76,77] Additional surface treatment and roughening steps of the n-side substrate can further increase the light extraction efficiency of the device up to one order of magnitude for bulk flip chip far-UVC LED designs.[78,79] Transparent p-side materials could increase the light extraction even further by adding a reflective layer between the submount wafer and chip and reflecting the downward emitted photons back through the chip and out of the device again.

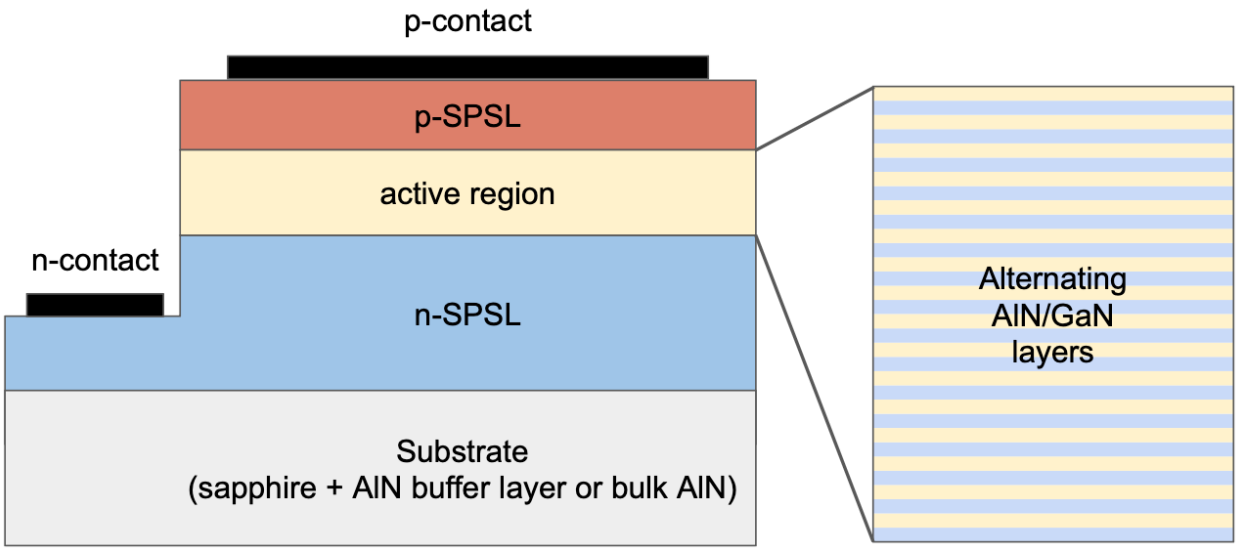

Figure 13: *SPSL LED schematic. Adapted from Nikishin 2018.*[82]

Short-period superlattice LEDs

A design variant of the traditional *p–i–n* MQW LED architecture that uses an alternative active layer design is the short-period superlattice (SPSL) LED.[80-82] Here, the active region does not comprise several nanometer-sized AlGaN/AlN MQWs, but hundreds of alternating AlN and GaN layers, each 1–5 atom layers thick (**Figure 13**).[82–84] Band gap and conductivity of the SPSL can be tuned via the layers' thickness.[85,86] This SPSL structure favors TE over TM emission, increasing light extraction efficiency.

SPSL far-UVC LEDs are developed[62], manufactured, and sold by Silanna UV, primarily for gas sensing applications. Their 236 nm LEDs have reached outputs of up to 18 mW in the lab—an approximate 1-year development advantage over conventional LED architectures of similar wavelengths—while their commercially available, lifetime-optimized LEDs output <1 mW.[87] Ultimately, however, Silanna UV does not consider SPSL LEDs as intrinsically superior to MQW LEDs, and both designs will reach similar, material-determined performance ceilings.

Nanowire LEDs

A structurally different design, the nanowire LED (NW-LED), addresses multiple difficulties of planar LEDs. First sold in 2015, NW-LEDs are a relatively novel structural variant of traditional LEDs.[88] Rather than layer materials being grown in contiguous planar layers, they may be radially stacked on top of each other (stacked nanowires) or around each other (core–shell nanowires), in either a forest of dense and thin wires or in an epitaxially predetermined arrangement (**Figure 14**).

Due to their small volume, individual nanowires are less sensitive to crystal impurities and strains from mismatching crystal lattices. The emitting surface area can also be up to 10 times larger than in conventional planar LEDs, which improves light extraction. A prototype of a far-UVC NW-LED was presented in 2017, which did not use a conventional *p–i–n* AlGaN LED design but 200x50 nm long nanowires comprising unalloyed n-GaN and n-AlN on the n-side, AlN as the active region, and hexagonal boron nitride (h-BN) as the p-side.[67] The device emitted between 210 and 220 nm, but

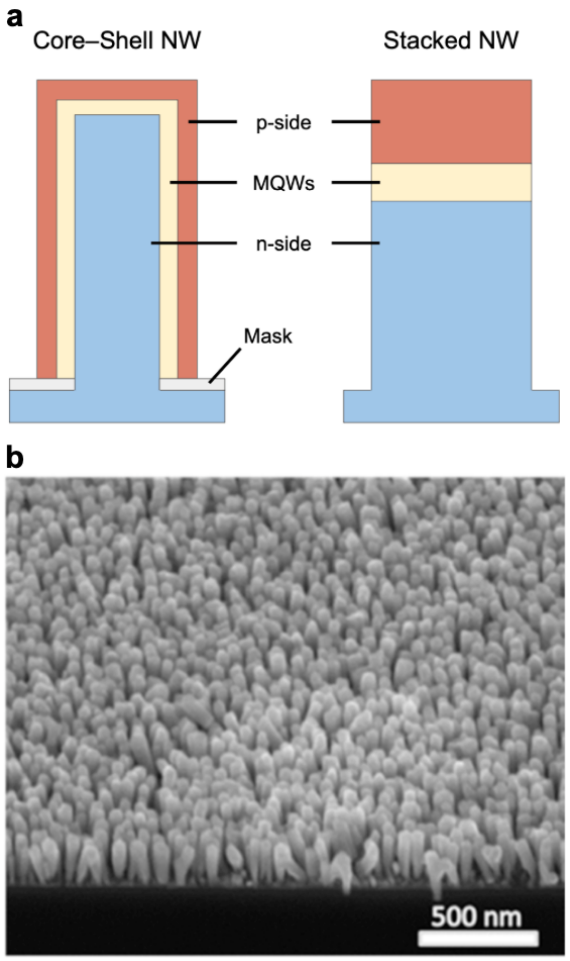

Figure 14: (a) *Structural comparison of core–shell nanowires and stacked nanowires.* ***(b)*** *Scanning electron microscope image of a stacked nanowire array, reprinted from Laleyan et al. 2017 with permission.*[67]

the total output of the prototype was low (50 nW), and the EQE was not reported. However, the authors presented it as a proof-of-concept for successful AlN/h-BN heterostructures with sizable advantages over p-doped AlN: h-BN is transparent to far-UVC photons, thus potentially increasing η_{ext} drastically, and p-type h-BN (with boron vacancies) injects holes more efficiently into the active region than p-AlN, thus improving the IQE.

Diode lasers

Until recently, UVC LEDs were insufficiently powered to achieve lasing. In 2019, the first edge-emitting UVC laser diode, emitting at 272 nm, was demonstrated.[89] Output power has increased over the years, but the sharp efficiency drop-off below 250 nm has so far precluded far-UVC laser diodes. But even ahead of full lasing, far-UVC LEDs can potentially be cavity-enhanced to narrow the emission spectrum and reduce emission outside the far-UVC spectral band, improving power output and spectral purity.[90]

4.2. Second-harmonic generation

Most viable approaches for solid-state far-UVC are native electroluminescent devices on the AlGaN material platform. The one alternative is in second harmonic generation (SHG) devices. SHG is a photon upconversion process that converts coherent light to twice its initial energy and half its initial wavelength–such that far-UVC light can be produced from a blue laser.

4.2.A Background

Discovered in 1961, SHG is now commonly used in applications where direct electroluminescence is difficult to achieve, e.g., in green laser pointers. Nonlinear crystals like potassium dihydrogen phosphate or ammonium dihydrogen phosphate have been used for SHG in the UVB and near-UVC region since the early 1970s.[91] In 1985, researchers achieved SHG in the far-UVC region using β-BaB_2O_4 (BBO) crystals.[92] BBO allows tunable SHG from 205–310 nm, though the conversion efficiency in the far-UVC region was reported to be low (10%) in early experiments with high-powered pulsed XeCl lasers.[93] The increased interest in far-UVC air disinfection during the COVID-19 pandemic led researchers to revisit SHG approaches using frequency-tripled, pulsed Nd:YAG crystal lasers, though conversion efficiencies were only slightly higher (16%), despite 7 ns pulses at a peak power density of 82 MW/cm². Overall, these and similar setups were complex and impractical.[94,95]

It has been proposed that using a blue GaN laser diode and a nonlinear optical element could solve complexity issues and might enable compact solid-state far-UVC sources, especially if the laser diode and nonlinear material are monolithically integrated on a single chip.[96] Such photonically integrated circuits (PICs) have been proposed with both BBO and AlN, sometimes utilizing an integrated micro-ring resonator.[97–101] Early experimental setups with separate diodes and BBO crystals were already quite compact but suffered extremely low conversion efficiencies (0.01%).[102]

A recent experiment with a continuous-wave blue laser diode coupled to a SiN/BBO waveguide has demonstrated the approach's viability.[103] However, the conversion efficiency was not reported, due to the overall low far-UVC output and issues with the calibration the far-UVC detector.

4.2.B Challenges and prospects

Compared to the widely used, established frequency-doubled lasers of longer wavelengths, SHG with blue lasers into the far-UVC is an emerging technology. Major questions will likely include:

1. Coupling efficiency: Most importantly, the performance of a frequency-doubled laser strongly depends on controlling and limiting optical losses. The laser must be efficiently coupled to the nonlinear

optical element, which needs a high conversion efficiency with little absorption, and the resulting far-UVC laser beam needs to be diffused or scattered without additional losses.

2. Temperature dependence: The device temperature and the temperature difference between the laser diode and nonlinear optical element must be carefully managed. SHG requires precise phase matching, and the temperature-dependency of the laser's emission wavelength could reduce coupling and conversion efficiency.

3. Laser safety standards: As the device's final or intermediate output will be a >1 mW invisible far-UVC laser beam, additional safety standards might be required for operation in occupied areas.

4. Manufacturability: The device may require additional, expensive manufacturing steps compared to a more straightforward LED design. The cost structure might be similar to that of LEDs as it also scales with the device area, but the additional cost of the nonlinear optical element and laser diode is unclear and might make a device uncompetitive.

On the other hand, a blue laser diode-based SHG far-UVC device could have several advantages over AlGaN LEDs:

1. Blue laser tech maturity: Blue lasers emitting at 450 nm are well-developed and—with WPEs above 50%—much more efficient than electro-luminescent UVC devices.

2. Very high spectral purity: The emission spectrum is extremely narrow, targeting the optimal disinfection wavelength and eliminating the need for far-UVC bandpass filters.

3. Relatively low conversion efficiency requirement: Conversion efficiency only needs to be moderately high. When coupled to a 50% efficient blue laser, a conversion efficiency of 20% would already result in a far-UVC emitter with 10% WPE, an order of magnitude more efficient than state-of-the-art far-UVC LEDs. But the SHG conversion efficiency can potentially be quite high (>90% energy efficient) when designed and integrated properly with the laser.[104,105]

4. Reliability: The device could be more reliable than far-UVC LEDs, which suffer from degradation and low lifetimes. Blue lasers already achieve lifetimes in the thousands of hours, but the lifetime of the SHG components has not been extensively studied. Based on

other SHG applications, one might expect little degradation as the SHG elements are electrically passive and generate little heat.

5. **High ceiling for growth:** The device would benefit from performance improvements to blue lasers and strategies that increase the laser's field intensity, such as resonators or pulsed operation.

6. **Easy miniaturization:** The device could be miniaturized to a form factor that behaves like an LED: flexibly integrable into diverse fixtures without requiring bulky electronics.

4.3. Other approaches

4.3.A Cathodoluminescent devices

Cathodoluminescent (CL) semiconductor devices, in which impact ionization from electron beams creates the electron–hole pairs in the device's active region, are another possible far-UVC emitter design.

CL devices can take advantage of materials with high IQE but are unsuitable as electroluminescent devices otherwise. As CL devices don't require electrical contacts, they work relatively well with materials with poor electrical efficiency. As they don't require any additional layers of materials besides the active region where electron-hole pairs recombine, they avoid issues with poor light extraction Electron-beam pumped AlGaN MQWs, for example, can achieve much higher WPE than comparable LED designs.[106,107] CL far-UVC emitters, using magnesium zinc oxide or hexagonal boron nitride, for example, are also much closer to commercialization than AlGaN LEDs or SHG devices, as few engineering problems need to be solved.[108–110] They also generate less RF interference.

However, CL devices are fundamentally more limited than LEDs or SHG with lasers. Miniaturized chip-scale electron-beam sources are still in early development and require vacuum compartments and high voltages.[111] Furthermore, electron-beam sources and impact ionization are less efficient than electroluminescence, fundamentally limiting WPE. Impact-ionization can also degrade some luminescent materials more quickly, limiting their lifetime. While electron-beam-pumped MQW structures are susceptible to defect accumulation, powdered phosphors—e.g., found in

CRT monitors—can last tens of thousands of hours.[112,113]

Overall, CL devices might be the first solid-state far-UVC emitters achieving KrCl excimer lamp performance levels. Still, their limitations compared to electroluminescent devices will likely render them obsolete within a decade.

4.3.B Alternative semiconductor materials

AlGaN is the most mature and developed ultra-wide band gap semiconductor material for RF and EL devices, but not the only one. Any semiconductor material satisfying the following criteria might be suitable for an electroluminescent far-UVC emitter:

1. **Band gap:** An electron band gap of 6.2–5.3 eV is required to emit in the far-UVC range (200–235 nm). Many ultra-wide band gap materials have been discovered or computationally predicted that fulfill this criterion, often nitrides or oxides.[114] Furthermore, a **direct band gap** is required for efficient EL. In indirect band gap materials, the momentum-mismatch between the conduction and valence bands favors non-radiative electron–hole recombinations, wasting energy as heat without photon emissions. A direct band gap aligns the minimum conduction band energy with the maximum valence band energy in momentum space, allowing vertical electron transitions that readily produce photons.[115]

2. **Bipolar transport:** The conduction of both electrons and holes, is critical in materials for EL. Efficient radiative recombination across the device's p–n junction requires that both electrons and holes be injected and reach the active region. Unipolar transport would lead to an imbalance between electron and hole densities, preventing efficient radiative recombination. Furthermore, accumulating one type of carrier over the other induces internal electric fields that reduce injection rates. To achieve a device with high WPE, the material must be sufficiently p- and n-type dopable to provide high mobilities for both negative electrons and positive holes, allowing equal bipolar conduction. Engineered heterostructures and doping profile designs can promote bipolar transport by enhancing electron and hole injection efficiencies.[116]

3. **Ability to form alloys and heterostructures:** Alloying with different compositions enables band gap engineering to tune the emission

wavelength, just as with AlGaN.[117,118] Additionally, heterostructures of different alloys allow further tuning of electrical and optical properties, for example, by inserting carrier-blocking layers.[119] Overall, the flexibility provided by alloys and heterostructures enables the optimization of emitter design, and a promising semiconductor material must have alloy capabilities to implement these heterostructure engineering concepts.

Other desirable but secondary criteria include good thermal conductivity to dissipate heat and prevent self-heating, thermal stability, and material abundance for cheap, scalable device production.

Boron nitride

After AlGaN, the second most frequently discussed ultra-wide band gap nitride semiconductor for far-UVC emission is boron nitride (BN). BN has different crystal structures, two of which are of importance here: hexagonal BN (h-BN) and cubic BN (c-BN). In h-BN, the most stable and common form, the 3D crystal comprises 2D sheets of BN, similar to graphite, whereas in c-BN, the crystal structure is analogous to diamond (**Figure 15**).[120] BN can also exist in an amorphous form without any regular crystal structure (a-BN) or in a rare wurtzite crystal structure (w-BN). The hexagonal form is easily growable with MOCVD or MBE on a wide range of surfaces—quartz, sapphire, copper, nickel, platinum, and other crystalline III-nitrides—whereas the synthesis of the cubic form is more difficult and requires high pressure and temperature.[121–124]

Though modeling suggested that h-BN's band gap was indirect, experiments in the early 2000s found strong 215 nm cathodoluminescent emission from h-BN, indicative of a direct band gap around 5.8 eV—and thus highly relevant for far-UVC optoelectronic devices.[125–127] Two-

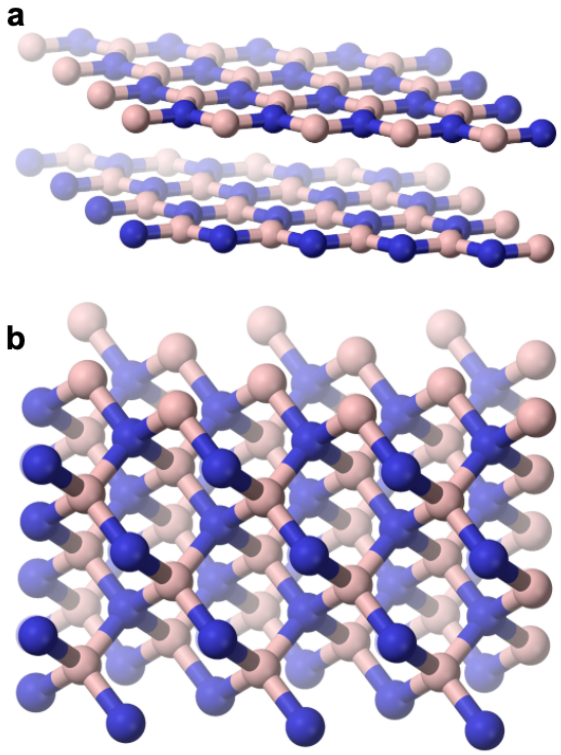

Figure 15: *Crystal structure of* ***(a)*** *hexagonal boron nitride and* ***(b)*** *cubic boron nitride.*[120]

photon excitation experiments ultimately confirmed an indirect band gap at 5.96 eV, corresponding to a 208 nm emission, and further studies attributed the (for an indirect band gap material surprisingly) high luminescent efficiency to strong exciton–phonon coupling and flat exciton dispersion.[128-130] In comparison, c-BN is experimentally less well characterized. Measurements indicate an indirect band gap at 6.36 eV, corresponding to a 195 nm emission wavelength, without the uncharacteristic luminescent behavior displayed by h-BN.[127]

BN can be employed in far-UVC emission either by enhancing AlGaN devices, or as its own native device.

1. Enhancing the performance of AlGaN devices by alloying them with and utilizing select characteristics of h-BN:

One of the large pitfalls of AlGaN devices is the difficulty of p-doping high-Al AlGaN and the resulting low IQE. This can be ameliorated by substituting the p-(Al)GaN side with p-type h-BN. Growing h-BN in a nitride-rich environment introduces boron vacancies, which inject holes much more efficiently than p-doped AlGaN. The h-BN layer also acts as a transparent electrode material. This design has been successfully implemented in AlN/GaN/h-BN nanowire LEDs emitting at 210 nm.[67] It was also proposed for

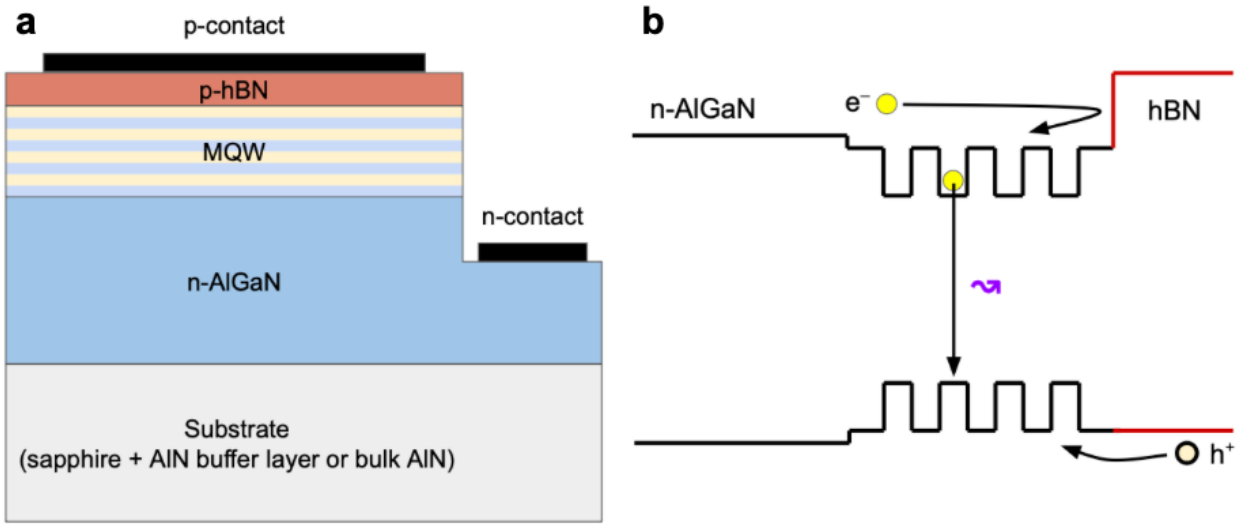

Figure 16: (a) *LED design using p-type h-BN instead of p-type AlGaN for hole injection and as an electron-blocking and p-contact layer.* ***(b)*** *The energy band diagram corresponding to such a p-type h-BN AlGaN LED. Electrons are blocked by the h-BN, while holes are easily injected into the active MQW region. Adapted from Maity et al. 2021.*[124]

traditional planar MWQ LED designs (**Figure 16**).[124]

An h-BN buffer layer between the substrate wafer and the AlGaN device can also reduce the threading dislocation density (TDD) of the AlGaN layers, thus improving light extraction and lifetime of the LED. The substrate and h-BN can then be removed, resulting in a thinner finished AlGaN flip-chip device with improved light extraction efficiency.[122,131,132]

2. Native bulk h-BN devices:

Despite its indirect band-gap, h-BN has many desirable properties as a far-UVC optoelectronic material. It has good far-UVC transparency, predominantly TE emission modes, a high exciton binding energy of over 700 meV, and strong exciton–phonon coupling, all positive signs.[124]

However, it is not especially suitable for electroluminescent devices, primarily due to doping challenges, which are even more severe h-BN than in AlGaN.[67,134] N-type doping has proven especially difficult, and the complex strategies required to achieve it at all are still in an early stage.[135]

Despite its unsuitability as a native LED material, its other desirable properties make h-BN a good candidate for integration with cathodoluminescent devices.

A demonstration unit of a handheld, battery-powered CL device with powdered h-BN, emitting at 225 nm, was even demonstrated in 2009, though the total output only reached 200 μW with an overall WPE of far below 1%.[133]

CL devices with bulk h-BN are primarily desirable for wavelength targeting, as they would be capable of emitting between 210-220 nm, a range of far-UVC currently not addressable by either excimer lamps and not likely to be reached by AlGaN devices.

3. Native bulk c-BN devices:

Of the three uses for BN in far-UVC emission, bulk c-BN devices are the most speculative, as it is the most difficult to grow and worst-charcterized BN phase. Available synthesis methods for c-BN require high pressures and temperatures, and result in a poly-crystalline powder of various BN phases, rather than a single crystal of c-BN.

As a result, many of the characteristics that make the indirect h-BN band gap viable for luminescence are either

absent or still undiscovered in c-BN, making it potentially wholly unsuitable for optoelectronic devices. CL from millimeter-sized beryllium-doped c-BN crystals only exhibited a broad spectrum from 240–400 nm without far-UVC emission.[136,137] Whether the large band gap can even enable tunable far-UVC emission closer to 200 nm remains an open question. Novel synthesis methods are being developed and will hopefully enable researchers to answer some of the open questions about c-BN's luminescent properties.

Ultra-wide band gap perovskites

Perovskites are a class of materials with a crystal structure similar to the mineral perovskite, calcium titanium oxide ($CaTiO_3$). They have the chemical formula ABX_3, where A and B are cations of different sizes, and X is an anion. The ideal cubic structure has the B cation in 6-fold coordination with a surrounding octahedron of anions X and the larger A cation in 12-fold cuboctahedral coordination (**Figure 17**).[138]

This versatile structure allows for numerous chemical substitutions on the A, B, and X sites, giving rise to a wide range of perovskite compounds with wide applications in electronics, catalysis, or high-temperature ceramics.[139,140] Perovskite raw materials are cheap, can be solution-processed, and exhibit favorable optoelectronic properties, such as high conversion efficiencies, tunable band gaps, defect resistance, long carrier diffusion lengths, and even semitransparency.[141,142] In recent years, intense research interest has been focused on using organic–inorganic hybrid perovskites as the active layer in high-efficiency solar cells, but these properties also make them interesting as LED materials, especially for displays. Red and green perovskite LEDs (PLEDs) based on hybrid perovskites show promising performance, though metal–halide perovskites with the wide band

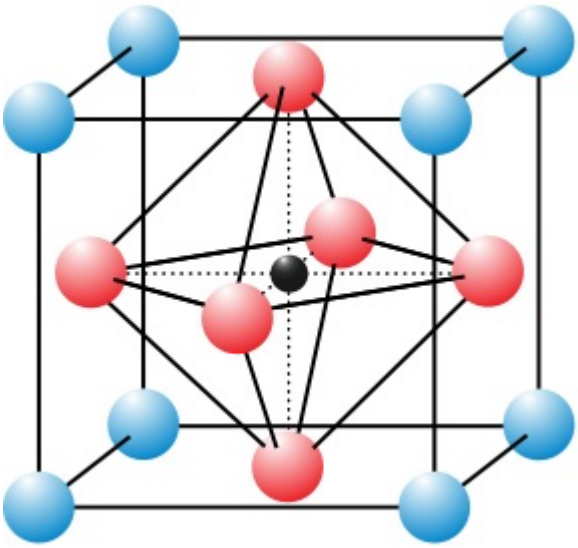

Figure 17: *Perovskite crystal structure with the larger cation A in blue, the smaller cation B in black, and the anion X in red.*[138]

gap required for blue light emission (>3 eV) lag relatively behind.[143,144]

Importantly, the perovskite space is largely unexplored. Computational searches for PLED candidates have been performed, but as most perovskite research interest is in solar cells, wide and ultra-wide band gap (UWBG) perovskites are usually excluded from the results. A systematic *in silico* search for UWBG perovskites using density functional theory (DFT) may yield useful candidate materials in the far-UVC.

Though it is wildly uncertain whether these candidate materials even exist, let alone have other desirable electroluminescent properties, the prospect of an inexpensive, easily producible, and defect-resistant far-UVC semiconductor material warrants a systematic investigation of this material class.

Oxides

Oxide semiconductors often have wider band gaps than their nitride or carbide counterparts. Many materials are now being explored for more efficient RF and power electronic devices. Gallium oxide (Ga_2O_3), for example, has a band gap of 4.7–4.9 eV (λ = 264–253 nm) compared to the 3.4 eV band gap of GaN. Similarly, the up to 7.6 eV band gap (λ =163 nm) of aluminum oxide (Al_2O_3) is so large that it is commonly used as an insulating barrier in capacitors. Aluminum gallium oxide (AGO) alloys could certainly reach the far-UVC band gap of 5.3–6.1 eV with much smaller aluminum fractions than AlGaN. Unfortunately, AGO has an indirect band gap, cannot be p-type or polarization doped, and exhibits extremely poor hole mobility, making it an unsuitable material for EL devices.

Other oxide material systems have better prospects for improvement. Rutile germanium oxide (r-GeO_2) is predicted to have ambipolar dopability, high carrier mobility, and higher thermal conductivity than Ga_2O_3, and might be a candidate material for future UWBG semiconductor devices, potentially in alloys with the recently-predicted rutile silicon dioxide (r-SiO_2).[145,146]

Balance-of-system

The challenges associated with creating and manipulating high-energy photons create a demand for materials with interesting optical properties in the UV region. Even materials not suitable for far-UVC electroluminescence might find uses in other parts of a far-UVC

device. Applications might be found throughout balance-of-system components and include:

1. Filters: The dichroic quartz/hafnium oxide filters used in existing KrCl excimer lamps constitute a significant part of the total device cost. Worse, their performance is strongly angle-dependent. Absorptive band-pass filters for the far-UVC region are still in early development and have not yet found commercial use. Durable and cheap absorptive filters would reduce the cost of both excimer lamps and solid-state devices with emissions outside of the far-UVC region, e.g., ~230 nm LEDs.

2. Encapsulants and light extraction strategies: Device encapsulations protect the semiconductor chip and shape the emission cone. They must be:

A. *Far-UVC transparent*.
B. *Long-term stable* (i.e., not yellowing or clouding).
C. Have a *matching refractive index* with the semiconductor material to maximize light extraction.

High thermal conductivity and stability with a low thermal expansion coefficient are also desirable, especially given the low WPE of existing and foreseeable solid-state far-UVC devices. It must also be assessed whether established LED light extraction strategies, such as photon recycling or surface nano-structuring, work with the available far-UVC compatible materials. The same applies to lenses and reflective coatings, which play an important role in light extraction and beam shaping.

3. Contacts: The ohmic contacts through which a current is applied to the top and bottom of the semiconductor chip must block as little of the generated photons as possible. To maximize light extraction from the chip, the contact material should be far-UVC-transparent on the emission side and far-UVC-reflective on the opposite side. Furthermore, the contact material needs to have a low resistance to minimize the required operating voltage and heat generation.

4. Integrated sensors: Cheap far-UVC sensors would be an extremely useful addition to any far-UVC lamp. They would not only indicate whether the device is operating but also whether the device is delivering the correct dose or whether degradation or defects have appeared. Real-time dosing information is especially important for standardized operation and ease of mind for the operator. Current far-UVC

sensors are mostly based on AlGaN photodiodes, costing up to tens of dollars. Cheaper and simpler designs would further decrease the total costs of far-UVC lamps.

5. Other components: Critical components like the LED power supply or heat sinks might also benefit from next-generation materials. The expected lower efficiency of solid-state far-UVC emitters requires efficient driver electronics and capable thermal management systems to keep the device at a comfortable temperature and prolong its lifetime. Oxide semiconductors and BN are already candidates for next-generation RF devices, and their development will eventually improve solid-state emitters in general, including far-UVC sources.

5. Forecasting

5.1. Summary of forecasting outcomes

The central activity of the workshop was a forecasting exercise, during which the participants assigned date ranges to the performance milestones. The forecasting results (**Table 3**, **Figure 18**, **Figure 19**, and **Figure 20**) were the basis of subsequent discussions as they both demonstrated some clear consensus views, as well as highlighted disagreements and uncertainties among the participants. Concretely, for every far-UVC emitter approach, every target metric, and every performance milestone (36 in total), participants gave the most likely year, the earliest plausible year, and the latest plausible year of achieving that milestone. The date range was operationally defined as the 90% confidence interval, meaning that participants are 90% sure that the milestone will be reached within their estimated time period. Additional visualizations of the forecasting results and the full tables can be found in the **appendix**.

Overall, three observations stood out particularly in the forecasts and the discussions:

1. Cathodoluminescent devices (CL devices) can already reach the phase 1

performance milestones today and may reach phase 2 milestones by 2025.

2. Devices based on second-harmonic generation (SHG devices) are expected to first reach the phase 3 performance milestones, possibly within the next five years.

3. Electroluminescent AlGaN-based devices (EL devices) were considered the safest bet for eventual high-performance emitters due to their established platform and experienced research community.

Table 3: *Mean results of the forecasting exercise. Bold entries indicate the* earliest *most likely year forecast for the given milestone.*

Target	**Milestone**	**CL devices**: *Most likely year (earliest plausible–latest plausible)*	**SHG devices**: *Most likely year (earliest plausible–latest plausible)*	**EL devices**: *Most likely year (earliest plausible–latest plausible)*
Lifetime of at least...	1k h	**2024** (2024–2026)	**2024** (2024–2027)	2025 (2024–2028)
	10k h	2028 (2026–2036)	**2026** (2025–2030)	2028 (2026–2032)
	25k h	2037 (2030–2042)	**2029** (2026–2034)	2033 (2029–2039)
Wall-plug efficiency of at least...	1%	2026 (2024–2031)	**2025** (2024–2026)	**2025** (2024–2027)
	3%	2030 (2027–2038)	**2026** (2025–2029)	2028 (2026–2032)
	10%	2041 (2030–2049)	**2031** (2028–2036)	2033 (2030–2039)
Cost per milliwatt of at most...	$10	**2025** (2024–2031)	**2025** (2024–2034)	2026 (2025–2028)
	$1	2029 (2027–2038)	**2027** (2025–2036)	2029 (2027–2035)
	$0.10	2039 (2030–2047)	**2031** (2026–2040)	2034 (2032–2042)

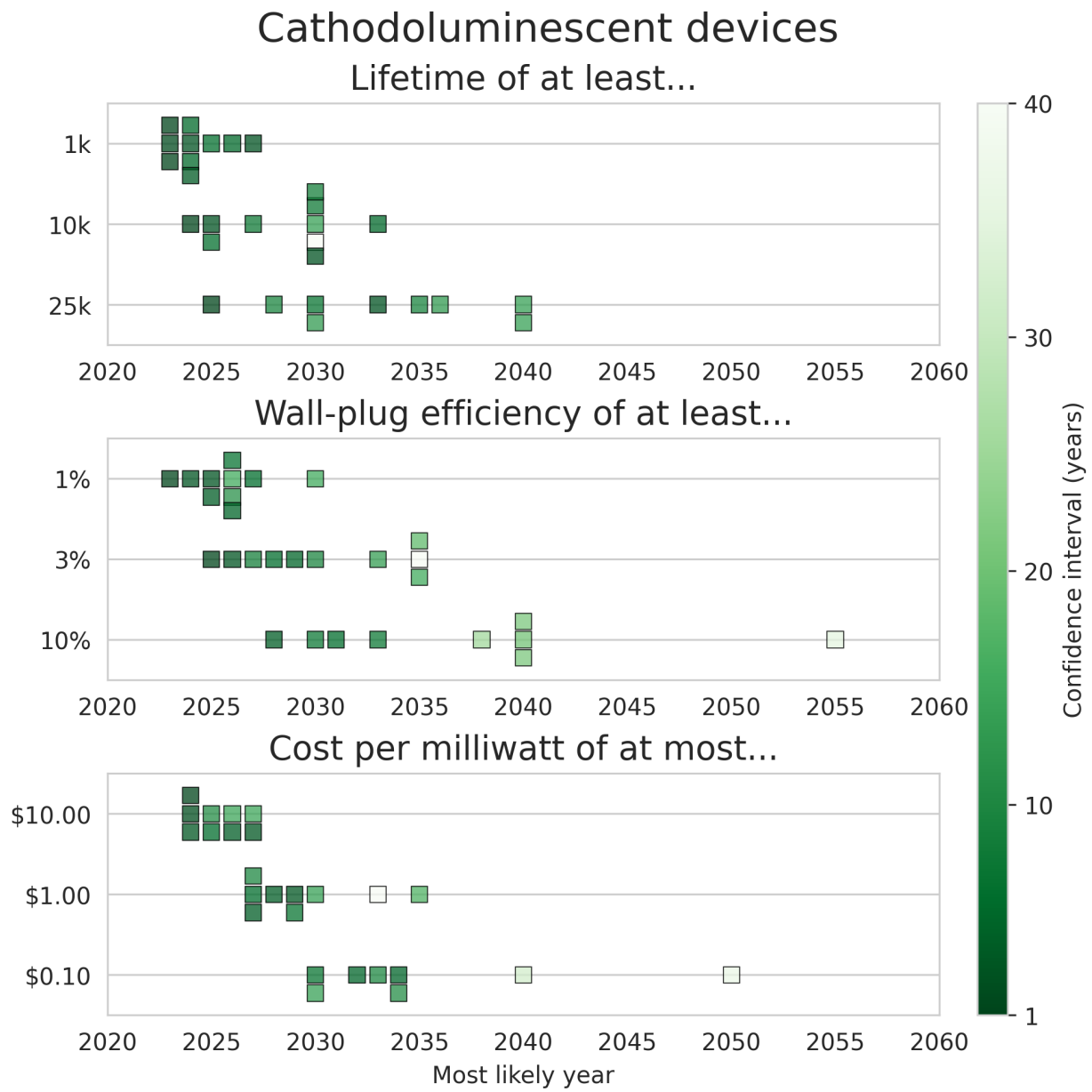

Figure 18: *Cathodoluminescent device forecasts. See* ***Supplementary Table 1*** *for details.*

The reason for the near-term optimism behind **CL devices** (Figure 18) is the relatively low barrier to emission. Bombarding a high-IQE material with electrons is technologically simple compared to designing and manufacturing an LED chip. Using a powdered material eliminates the need for a waveguide and improves light outcoupling efficiency while impact ionization circumvents the p-transport problem found in electroluminescent UV emitters. CL devices are, however, limited in their performance ceiling

compared to EL and SHG devices. To prevent oxidation, the material and electron source are enclosed in a vacuum package with a limited lifetime and limited miniaturization potential. Furthermore, impact ionization is much less efficient than p–n junctions in creating electron–hole pairs. Though early-stage commercial CL devices that emit in the far-UV with reasonable WPE are already available, it is substantially more challenging to achieve even somewhat spectrally pure far-UVC emission with CL at a WPE above single-digit percent. It was thus consensus that CL devices will likely not achieve phase 2 or 3 milestones.

SHG devices (Figure 19) show the most promise in the high-performance domain, and their forecasts exhibited the shortest time between the phase 1, 2, and 3 milestones. This is mostly due to the presumed singular bottleneck of nonlinear optical element integration that needs to be solved to achieve high output power with existing blue lasers.

The relatively unoptimized prototypes can already achieve phase 1 milestones today, and participants were confident that improvements will materialize quickly, leading SHG devices to reach phase 2 milestones in the coming 2–4 years and phase 3 milestones 1–2 years later. Forecasts on phase 3 milestones for lifetime and WPE were spread wider with lower confidence, as data on the long-term performance and ceiling of far-UVC nonlinear optical elements are not available yet. However, as degradation occurs primarily in the laser and inefficiencies of the SHG manifest mostly as unaltered blue light and not transformed heat, participants were generally optimistic that long lifetimes are achievable.

Recent developments of high-efficiency blue lasers also reduce the need for highly efficient SHG to achieve acceptable overall WPE. Participants considered WPEs of 2% commercializable and the phase 3 WPE of 10% plausible as a short-term goal achievable in a few years. Uncertainty about the cost floor and scalability of the fully integrated SHG system compared to a traditional LED remains and will ultimately be determined by semiconductor growth steps, yields, substrate size, device size, and related factors.

While the technological development of SHG devices has not followed the expected trajectory since the workshop, the milestones can still be achieved within their mean confidence intervals. It was also remarked that the

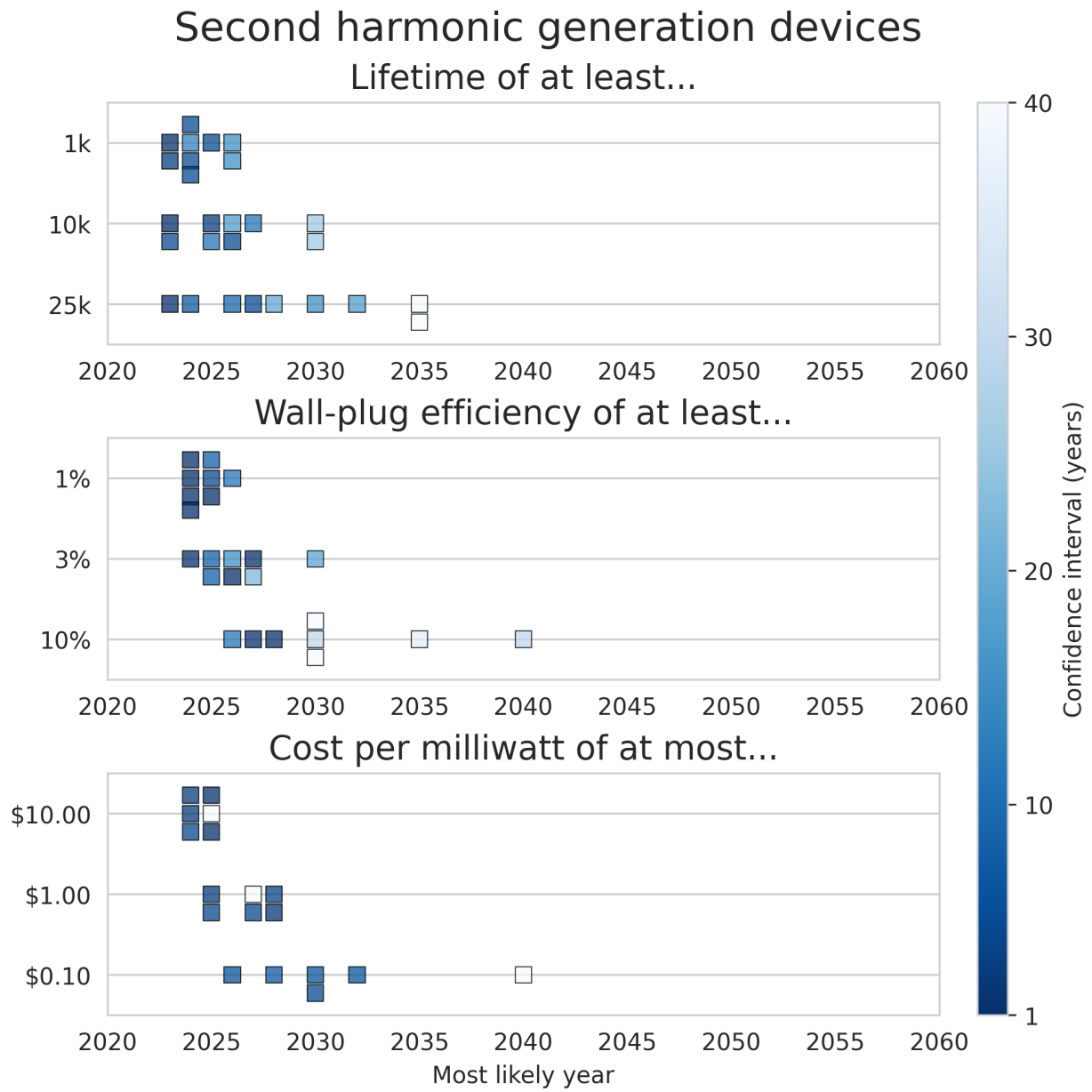

Figure 19: *Second-harmonic generation device forecasts. See* ***Supplementary Table 2*** *for details.*

comparatively optimistic SHG forecasts could possibly stem from a lack of experimental grounding at the time of the workshop and that a better-calibrated forecast with more academic SHG experts would have placed the SHG approach on a timeline similar to that of electroluminescent AlGaN devices.

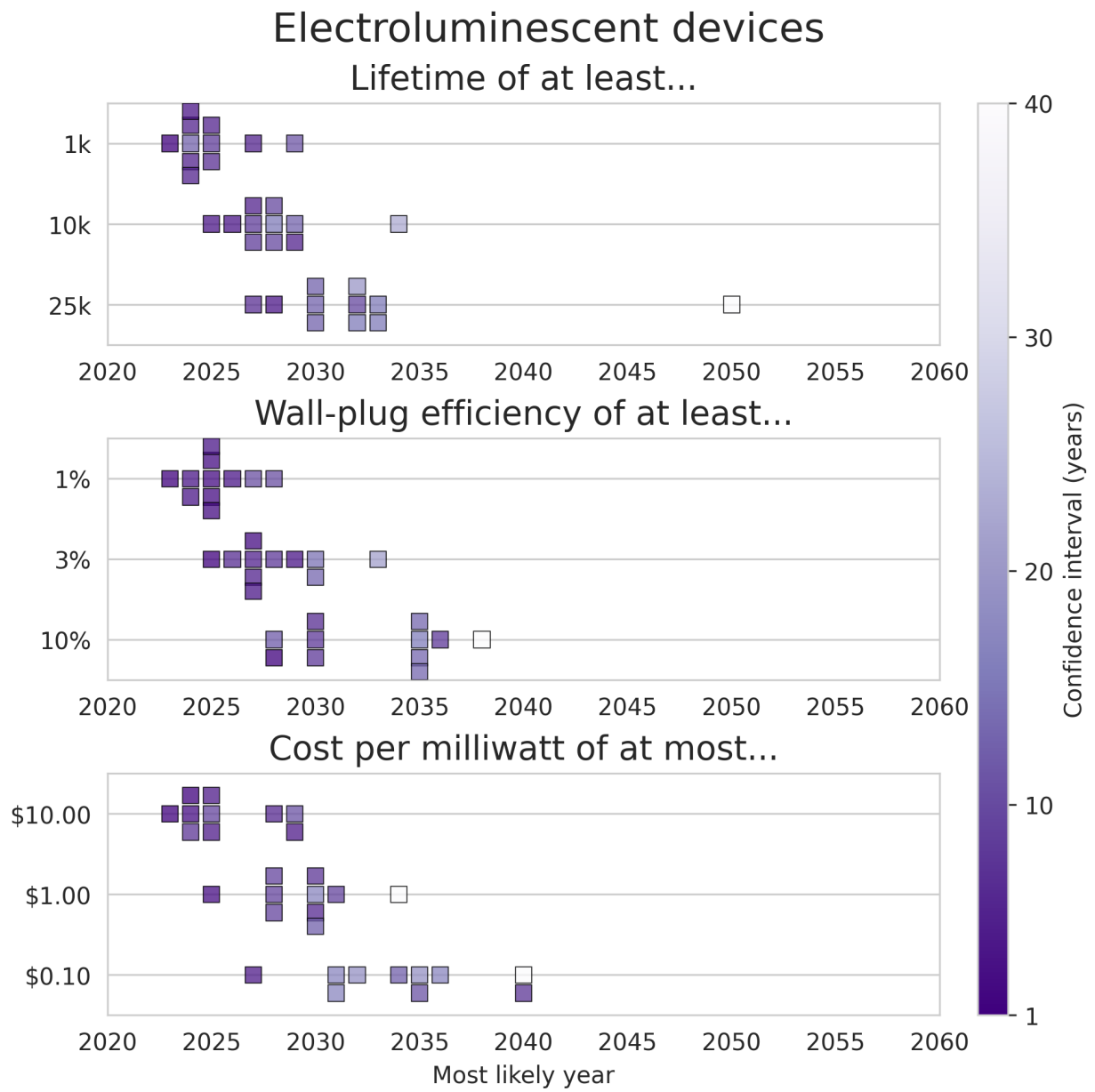

Figure 20: *Electroluminescent device forecasts. See* ***Supplementary Table 3*** *for details.*

On the **EL device** (Figure 20) performance milestones, participants agreed that phase 1 milestones are already achievable by today's far-UVC LED prototypes and that phase 2 and 3 milestones are theoretically achievable with the current AlGaN device platform, though later than with SHG devices. Participants expected EL devices to reach phase 2 milestones in 4–7 years and phase 3 milestones in ~10 years. In contrast to the SHG approach, EL devices need to solve more engineering challenges—p-doping,

light extraction, and point defect minimization—as outlined in **section 4.1.** These challenges were not considered insurmountable, but more research time is expected before the high-performance milestones are reached. Importantly, most participants considered the EL AlGaN devices to be the long-term most dependable pathway to high-performance solid-state far-UVC sources, even if SHG devices might reach performance milestones earlier. This results from long experience with the material platform, a well-characterized pro-duction process, and the high theoretical performance ceiling of LEDs. However, since the forecasting exercise did not query this aspect, it is not reflected in the results.

5.2. Limitations of the forecasting exercise

As with all predictions, these forecasts must only be considered with the underlying assumptions and limitations in mind.

First and foremost, solid-state far-UVC emitters are an emerging technology that is still comparatively early in its development. Forecasting performance milestones >5 years in advance is thus an inherently uncertain endeavor. Some extrapolations from Haitz's Law (the observation that cost per lumen and output per LED chip improve 10- and 20-fold, respectively, per decade) and the development curves of conventional 260–280 nm GUV LEDs are possible, but the realization or absence of fundamental research breakthroughs can shift the expected timelines drastically.

This uncertainty is confounded by the unpredictability of funding and market demand changes. Currently, the market for far-UVC lamps is largely nonexistent, resulting in little investments in emitter R&D. The forecasts assumed a 'business-as-usual' funding situation, in which a handful of academic labs and small startups and R&D groups continue with their research agendas. A sudden inflow of money and demand could principally cut timelines significantly by parallelizing research, especially for approaches that are not blocked by consecutive nodes in their tech tree, such as SHG devices. Conversely, a lack of funding in one area could greatly extend the timelines projected in the exercise, which only captures the opinions of those in the room at a moment in time.

Finally, the target metrics selected for the forecasts were underdefined and partially dependent on each other. As

seen in **section 3**, most of the metrics are influenced by other metrics and often trade-off. A high lifetime is easily achievable by running an LED at an impractically low current density, drastically reducing total output power and increasing cost per watt. Similarly, spectral control is attainable with expensive band-pass filters that slash WPE. When the target metrics are subject to direct tradeoffs, one milestone can be accelerated by slowing down another. Participants were asked to forecast without tradeoffs in mind, but given many of the open questions around optimal air disinfection wavelengths and price points acceptable for customer uptake, it is likely that such tradeoffs will be made in final products.

Given these limitations, the forecasts were understood as tools to identify common opinions and pinpoint disagreements among the participants. We believe that the assigned date ranges and rankings are directionally correct (e.g., SHG approaches having the potential to yield high-performance devices first) but would have lower confidence in determining the exact year in which a given milestone is achieved.

6. Conclusion

Given the limitations of KrCl excimer lamps and the variety of solid-state emitter approaches, the potential of solid-state far-UVC sources is clear: In the medium- to long-term, solid-state sources will outperform excimer sources while significantly reducing the cost of far-UVC emission.

In the short term (until 2026), cathodoluminescent devices could compete with current excimer lamps if sufficient demand would exist. In the medium term (2026–2030), second-harmonic generation approaches using blue lasers show promise due to the maturity of the blue laser diode and the low number of sequential, interdependent research bottlenecks, but they also have higher uncertainty associated with their ultimate competitiveness with regular LEDs. Such electroluminescent AlGaN devices—primarily, but not exclusively, LEDs—were estimated to be most likely to reach target milestones on a long-term time horizon (beyond 2030). LEDs benefit from lower manufacturing complexity and a higher efficiency ceiling, which can theoretically result in a lower cost per watt compared to all other device classes, but several open research questions on the fundamental limitations of AlGaN as a far-UVC emitter remain. Their resolution over the coming years will determine the future of the AlGaN device platform for far-UVC emission. Whether AlGaN LEDs or SHG devices will dominate the far-UVC emitter space in the 2030s and beyond remains to be seen.

6.1. Research & development priorities

Regardless of which technology will ultimately yield the highest-performance emitters we need, the workshop identified the most important research and development priorities for each approach. These priorities might overlap on some common challenges associated with far-UVC but are largely independent of each other.

In the short-term and for the CL-based approach:

1. **Improving packaging**: Adapting conventional vacuum-tube packaging techniques to be compatible with transitions between glass and far-UV-transmissive materials.

2. **Expanding available materials**: Like for LEDs, AlGaN, AlN, and BN, can be useful materials for CL devices. However, they must be optimized for cost and CL efficiency in ways that have not yet been done.

For the comparatively novel SHG-based approach, R&D must focus on both the laser and the nonlinear optical elements:

1. **Improving blue laser diodes:** While blue lasers are already quite efficient, expanding their wavelength tunability range would allow for wider coverage of the far-UVC spectrum.
2. **Integrate laser and SHG-element:** An on-chip integration of the laser and the nonlinear optical element is the required first step for gauging coupling, reliability, and conversion efficiency and for identification of follow-up research priorities.

For AlGaN devices, the most important R&D priorities are those that are general to many different device types, and the rest follow from the main efficiency bottlenecks:

1. **Understanding defects:** Defects, especially point defects, in the AlGaN crystal structure negatively affect IQE, device degradation, and reliability. But while threading dislocations have been largely characterized and managed, point defects remain poorly understood. It is thus crucial to precisely determine their effect on device efficiency, end-of-life performance, and failure and identify ways to minimize their presence. Only devices with minimal defects will achieve the high output power and long lifetimes that are outlined in **section 4.1.**
2. **Improving native AlN substrate:** While not a bottleneck of device efficiency per se, special consideration should still be given to the development of cheaper native AlN substrate, as this would also benefit SHG devices, along with a wider variety of AlGaN EL devices. Devices grown on native AlN exhibit fewer defects and require fewer production steps than devices grown on sapphire substrate. Continuing the development of native AlN wafers will make them competitive with sapphire for far-UVC devices requiring high quality and will also open up access to the highly scalable, existing 4–6" wafer production infrastructure.

3. **Improving light extraction:** Opportunities to improve the light extraction efficiency might be the most important findings for progressing far-UVC LEDs. Promising avenues for additional research include, for example, identifying far-UVC-transparent alloys for the device's p-side, increasing the device's emissive surface (e.g., by using nanowire LED designs or micro-LED arrays), or exploring LED designs that favor TE-emission (e.g., SPSL LED designs).
4. **Improving p-doping:** The low internal quantum efficiency of current far-UVC LEDs is chiefly limited by inefficient p-doping (and material defects; see point 4). Approaches to circumvent these doping difficulties are being explored—e.g., polarization doping or employing heterostructures with different materials as hole-injectors, such as hexagonal boron nitride (h-BN) or p-doped silicon (p-Si)—and need to be developed further. Achieving spectral peaks in the far-UVC region requires a degree of quantum well doping control and uniformity that has yet to be achieved, but the feasibility of which is demonstrated by the commercially available 260–280 nm GUV LEDs.
5. **Improving electrical efficiency:** Electrical efficiency is not the biggest bottleneck of overall efficiency, but it is still lacking. Finding opportunities to maximize it will become increasingly important as other efficiency limitations are being addressed. Concretely, the device n- and p-contact resistance must be improved, and the n-AlGaN and p-AlGaN current spreading layer resistance must be reduced. It should be noted that improvements in other parameters, e.g., better light extraction efficiency using UV-reflective metal contacts, might compromise the electrical properties, e.g., result in an increased contact resistance. These potential trade-offs need to be well-understood and optimized. To minimize efficiency droop at high current densities, LED designs with additional quantum wells help reduce Auger–Meitner recombination, and improved chip design, heatsinking, and packaging can reduce Joule heating.

The approach-independent R&D priorities listed below are not required for developing the emitters themselves but will be necessary for performant far-UVC lamp systems:

1. **Device encapsulation:** The cheap epoxy or silicone encapsulants that seal visible LEDs are usually incompatible with UV LEDs. The even shorter wavelengths and high thermal output of far-UVC LEDs pose additional

challenges. Long-term far-UVC-resistant, -transparent, and thermally stable encapsulants suitable for mass production must be developed to reduce costs and increase scalability.

2. **New materials:** Novel, far-UVC compatible materials can find applications in various balance-of-system components around the emitter, such as filters, packaging, and optics, or even new cathodoluminescent phosphors or nonlinear optical materials for SHG devices. Material scientists are continuously expanding the frontiers of known compounds, and comprehensive searches of those results can unlock important improvements in far-UVC lamp components.

6.2. Funding recommendations

When discussing the funding gaps of various approaches, participants considered the amount of funding necessary to make a material difference in accelerating the development of a given approach to be in the tens of millions of dollars. Such a financial boost would not necessarily solve all of the identified R&D priorities but would solve some and allow improvements on the others. The most important problem outlined by the participants was, however, not the lack of R&D funding; it was the absence of a market. Any transition to solid-state emitters—as observed in visible lighting or conventional GUV applications—is entirely dependent on the existence of *sufficient demand* to take advantage of the scaling potential. If demand for far-UVC sources remains low, solid-state far-UVC is less attractive, given the much greater research and capital requirements. Furthermore, many of the R&D priorities were not considered fundamental research problems that require a moonshot program to solve but concrete engineering challenges with often promising potential solutions available. Participants were convinced that investment into hardware R&D would materialize with demand from a demonstrated market. Almost all the funding recommendations and wishes discussed at the workshop thus revolved around market-shaping and the issue of kickstarting demand.

We recommend funding three different categories:

(a) Non-emitter research of data gaps and hardware:

1. **Safety & effectiveness research:** Most of our current knowledge of far-UVC comes from limited, usually small-*n* experimental research and modeling studies. Though it is an extremely promising technology based on first principles and early data, substantial knowledge gaps remain. On far-UVC safety, we recommend funding the research agenda outlined in *"Assessing the safety of new germicidal far-UVC technologies"* by Görlitz et al., 2023.[18] On far-UVC effectiveness, we recommend funding multiple studies with infection endpoints that quantify the effect of far-UVC air disinfection in diverse real-world scenarios.
2. **Infrastructure technology:** For consumers to adopt a new technology, it needs to be easy to use. Funding should be directed to developing infrastructure technology that will make installation, operation, and validation of far-UVC systems as frictionless as possible. This includes products like modeling software that allows architects and building managers to easily plan far-UVC installations or lamp-accompanying sensors for validating installations.
3. **New science models:** In the absence of organic demand or substantial government or philanthropic funding, there is often little incentive for companies, venture capital firms, or other for-profit ventures to fund the development of, e.g., infrastructure technology or fundamental mechanistic research. While some of this research may interest academic labs, funding incentives or engineering capacities often prove prohibitive. New science models like Focused Research Organizations (FROs) or Industry-University Cooperative Research Centers (IUCRCs) that can operate outside of the traditional research incentive constraints provide a promising avenue and should be considered.

(b) Developing legitimacy:

4. **Public acceptance research:** Little is known about the public's attitude towards far-UVC air disinfection. It is important to fund public acceptance research early to understand the questions and worries that the public has and to identify the framings of the technology that will be accepted. Public opinion is often used by incumbents to prevent the adoption of new technologies, as could be seen with, for example, the war of the currents, cadmium-containing quantum dot televisions, or electric cars. A technology as potentially impactful as far-UVC air

disinfection should avoid past mistakes and gauge (and engage) the public early.

5. **Standards development:** After addressing the knowledge gaps and public acceptance around far-UVC, funding should be directed towards an independent, non-industry-led far-UVC air disinfection standard that lamp manufacturers, consumers, and academic experts agree on. Any standards committee or organization should engage all relevant standards and certification agencies to avoid conflicting standards and future confusion. It will be crucial for the standard to establish a legible "value per watt"-metric that integrates and quantifies the provided value of disease prevention from a far-UVC air disinfection installation.

(c) Market-shaping:

6. **Market research:** To kickstart demand, funding should be directed towards a detailed market analysis to identify potential beachhead markets for far-UVC systems. Whether done with private or public funding, the insight should be shared openly to benefit the whole industry, as beachhead markets can be used to gather data from larger studies that would otherwise be intractable. This can serve as a particularly potent demand stimulant when combined with advance market commitments.
7. **Advance market commitments:** Advance market commitments can help negotiate the gap between potential sales and necessary investments. With the promise of a secured market, developers can more confidently fund the necessary R&D, potentially leading to quicker commercialization. Such commitments can be instrumental in transitioning far-UVC LEDs from experimental stages to widespread, practical use. Prizes awarded to the first competitors reaching a certain target product profile or production goal (such as the X- or L-Prizes) can similarly stimulate up-front investments.

7. Bibliography

1. Molinari, N.-A. M. *et al*. The annual impact of seasonal influenza in the US: Measuring disease burden and costs. *Vaccine* 25, 5086–5096 (2007).

2. Fendrick, A. M., Monto, A. S., Nightengale, B. & Sarnes, M. The economic burden of non-influenza-related viral respiratory tract infection in the United States. *Arch Intern Med* 163, 487–494 (2003).

3. Hellgren, J., Cervin, A., Nordling, S., Bergman, A. & Cardell, L. O. Allergic rhinitis and the common cold – high cost to society. *Allergy* 65, 776–783 (2010).

4. Institute for Health Metrics and Evaluation. Global Burden of Disease Study 2019. *Global Burden of Disease Study 2019 (GBD 2019) Data Resources* https://ghdx.healthdata.org/gbd-2019 (2020).

5. Bruns, R. & Teran, N. Weighing the Cost of the Pandemic. *Institute for Progress* https://ifp.org/weighing-the-cost-of-the-pandemic/ (2022).

6. Cutler, D. M. The Costs of Long COVID. *JAMA Health Forum* 3, e221809 (2022).

7. Cohen, L. E., Spiro, D. J. & Viboud, C. Projecting the SARS-CoV-2 transition from pandemicity to endemicity: Epidemiological and immunological considerations. *PLoS Pathog* 18, e1010591 (2022).

8. WHO. Ending the COVID-19 emergency and transitioning from emergency phase to longer-term disease management: guidance on calibrating the response, 4 September 2023. https://www.who.int/publications-detail-redirect/WHO-WHE-SPP-2023.2 (2023).

9. Casadevall, A. Pandemics past, present, and future: progress and persistent risks. *J Clin Invest* 134, (2024).

10. Millett, P. & Snyder-Beattie, A. Existential Risk and Cost-Effective Biosecurity. *Health Security* 15, 373–383 (2017).

11. Esvelt, K. M. Delay, Detect, Defend: Preparing for a Future in which Thousands Can Release New Pandemics. (2022).

12. Clemesha, W. W. The Use of Ultra-Violet Rays in the Sterilization of Water. *Ind Med Gaz* 47, 267–269 (1912).

13. Kowalski, W. *Ultraviolet Germicidal Irradiation Handbook: UVGI for Air and Surface Disinfection*. (Springer, Berlin, Heidelberg, 2009). doi:10.1007/978-3-642-01999-9.

14. Kleinwaks, G., Fraser-Urquhart, A., Kraprayoon, J. & Morrison, J. Air Safety to Combat Global Catastrophic Biorisk. *1Day Sooner & Rethink Priorities Report* (2023).

15. Nardell, E. A. *et al*. Safety of upper-room ultraviolet germicidal air disinfection for room occupants: results from the Tuberculosis Ultraviolet Shelter Study. *Public Health Rep* 123, 52–60 (2008).

16. Beck, S. E., Wright, H. B., Hargy, T. M., Larason, T. C. & Linden, K. G. Action spectra for validation of pathogen disinfection in medium-pressure ultraviolet (UV) systems. *Water Research* 70, 27–37 (2015).

17. Hessling, M., Haag, R., Sieber, N. & Vatter, P. The impact of far-UVC radiation (200–230 nm) on pathogens, cells, skin, and eyes – a collection and analysis of a hundred years of data. *GMS Hyg Infect Control* 16, Doc07 (2021).

18. Görlitz, M. *et al*. Assessing the safety of new germicidal far-UVC technologies. *Photochemistry and Photobiology* n/a, (2023).

19. Eadie, E., Barnard, I. M. R., Ibbotson, S. H. & Wood, K. Extreme Exposure to Filtered Far-UVC: A Case Study. *Photochem Photobiol* 97, 527–531 (2021).

20. Welch, D. *et al*. No Evidence of Induced Skin Cancer or Other Skin Abnormalities after Long-Term (66 week) Chronic Exposure to 222-nm Far-UVC Radiation. *Photochem Photobiol* (2022) doi:10.1111/php.13656.

21. Zamudio Díaz, D. F. *et al*. Skin optical properties from 200 to 300 nm support far UV-C skin-safety in vivo. *Journal of Photochemistry and Photobiology B: Biology* 247, 112784 (2023).

22. Buonanno, M. *et al*. 207-nm UV Light - A Promising Tool for Safe Low-Cost Reduction of Surgical Site Infections. I: In Vitro Studies. *PLOS ONE* 8, e76968 (2013).

23. Buonanno, M. *et al*. 207-nm UV Light—A Promising Tool for Safe Low-Cost Reduction of Surgical Site Infections. II: In-Vivo Safety Studies. *PLOS ONE* 11, e0138418 (2016).

24. Schuit, M. A. *et al*. SARS-CoV-2 inactivation by ultraviolet radiation and visible light is dependent on wavelength and sample matrix. *Journal of Photochemistry and Photobiology B: Biology* 233, 112503 (2022).

25. Welch, D., Aquino de Muro, M., Buonanno, M. & Brenner, D. J. Wavelength-dependent DNA Photodamage in a 3-D human Skin Model over the Far-UVC and Germicidal UVC Wavelength Ranges from 215 to 255 nm. *Photochemistry and Photobiology* 98, 1167–1171 (2022).

26. Sliney, D. H. & Stuck, B. E. A Need to Revise Human Exposure Limits for Ultraviolet UV-C Radiation †. *Photochem & Photobiology* 97, 485–492 (2021).

27. Kreusch, S., Schwedler, S., Tautkus, B., Cumme, G. A. & Horn, A. UV measurements in microplates suitable for high-throughput protein determination. *Analytical Biochemistry* 313, 208–215 (2003).

28. American Conference of Governmental Industrial Hygienists, Inc. Ultraviolet Radiation TLVs. (2021).

29. OSHA. OZONE | Occupational Safety and Health Administration. https://www.osha.gov/chemicaldata/9 (2024).

30. Collins, D. B. & Farmer, D. K. Unintended Consequences of Air Cleaning Chemistry. *Environ. Sci. Technol.* 55, 12172–12179 (2021).

31. Fox, J. ASHRAE 241 Control of Infectious Aerosols Part 4 – Safety and Effectiveness of Air Cleaners. *Medium* https://itsairborne.com/ashrae-241-control-of-infectious-aerosols-part-4-safety-and-effectiveness-of-air-cleaners-977ef88fc53a (2023).

32. Peng, Z. *et al.* Significant Production of Ozone from Germicidal UV Lights at 222 nm. *Environ. Sci. Technol. Lett.* (2023) doi:10.1021/acs.estlett.3c00314.

33. Peng, Z. & Jimenez, J. L. Evaluation of Secondary Chemistry due to Disinfection of Indoor Air with Germicidal Ultraviolet Lamps. 2022.08.25.22279238 Preprint at https://doi.org/10.1101/2022.08.25.22279238 (2022).

34. International Ultraviolet Association. Impact of UV-C on Material Degradation: Working Group. https://www.iuva.org/impact-uv-c-task-force (2023).

35. Bueno de Mesquita, P. J., Sokas, R. K., Rice, M. B. & Nardell, E. A. Far-UVC: Technology Update with an Untapped Potential to Mitigate Airborne Infections. *Annals ATS* 20, 1700–1702 (2023).

36. Mikszewski, A., Stabile, L., Buonanno, G. & Morawska, L. The airborne contagiousness of respiratory viruses: A comparative analysis and implications for mitigation. *Geoscience Frontiers* 13, 101285 (2022).

37. Goyal, A., Reeves, D. B. & Schiffer, J. T. Multi-scale modelling reveals that early super-spreader events are a likely contributor to novel variant predominance. *Journal of The Royal Society Interface* 19, 20210811 (2022).

38. Stein, R. A. Super-spreaders in infectious diseases. *International Journal of Infectious Diseases* 15, e510–e513 (2011).

39. Cassar, J. R., Mills, E. W. & Demirci, A. Characterization of pulsed light for microbial inactivation. *Journal of Food Engineering* 334, 111152 (2022).

40. Rufyikiri, A. S. *et al.* Germicidal efficacy of continuous and pulsed ultraviolet-C radiation on pathogen models and SARS-CoV-2. *Photochem Photobiol Sci* 23, 339–354 (2024).

41. Zou, X.-Y. *et al.* Enhanced inactivation of E. coli by pulsed UV-LED irradiation during water disinfection. *Sci Total Environ* 650, 210–215 (2019).

42. Pattinson, M. *2018 Solid-State Lighting R&D Opportunities*. (2019).

43. Pattinson, M. *et al. 2022 Solid-State Lighting R&D Opportunities*. https://www.energy.gov/sites/default/files/2022-02/2022-ssl-rd-opportunities.pdf (2022).

44. Akasaki, I. Key inventions in the history of nitride-based blue LED and LD. *Journal of Crystal Growth* 300, 2–10 (2007).

45. Amano, H. Development of GaN-based blue LEDs and metalorganic vapor phase epitaxy of GaN and related materials. *Progress in Crystal Growth and Characterization of Materials* 62, 126–135 (2016).

46. Amano, H., Sawaki, N., Akasaki, I. & Toyoda, Y. Metalorganic vapor phase epitaxial growth of a high quality GaN film using an AlN buffer layer. *Applied Physics Letters* 48, 353–355 (1986).

47. Amano, H., Kito, M., Hiramatsu, K. & Akasaki, I. P-Type Conduction in Mg-Doped GaN Treated with Low-Energy Electron Beam Irradiation (LEEBI). *Jpn. J. Appl. Phys.* 28, L2112 (1989).

48. Nakamura, S., Mukai, T. & Senoh, M. Candela-class high-brightness InGaN/AlGaN double-heterostructure blue-light-emitting diodes. *Applied Physics Letters* 64, 1687–1689 (1994).

49. Amano, H. *et al*. The 2020 UV emitter roadmap. *J. Phys. D: Appl. Phys.* 53, 503001 (2020).

50. Kobayashi, H. *et al*. Milliwatt-power sub-230-nm AlGaN LEDs with >1500 h lifetime on a single-crystal AlN substrate with many quantum wells for effective carrier injection. *Applied Physics Letters* 122, 101103 (2023).

51. Kobayashi, H. *et al*. Enhanced Wall-Plug Efficiency over 2.4% and Wavelength Dependence of Electrical Properties at Far UV-C Light-Emitting Diodes on Single-Crystal AlN Substrate. *physica status solidi (RRL) – Rapid Research Letters* n/a, 2400002 (2024).

52. Kneissl, M. External Quantum Efficiencies of UV-LEDs. www.tu.berlin/en/originagkneiss/research (2024).

53. Kolbe, T. *et al.* 234 nm far-ultraviolet-C light-emitting diodes with polarization-doped hole injection layer. *Applied Physics Letters* 122, 191101 (2023).

54. Chen, Y. *et al.* Review on the Progress of AlGaN-based Ultraviolet Light-Emitting Diodes. *Fundamental Research* 1, 717–734 (2021).

55. Liu, D. *et al.* 226 nm AlGaN/AlN UV LEDs using p-type Si for hole injection and UV reflection. *Appl. Phys. Lett.* 113, 011111 (2018).

56. Guo, Y. *et al.* High-Reflectivity Mg/Al Ohmic Contacts on n-GaN. *IEEE Photonics Technology Letters* 33, 347–349 (2021).

57. Sim, K.-B. *et al.* Optimization of Ni/Ag-Based Reflectors to Improve the Performance of 273 nm Deep Ultraviolet AlGaN-Based Light Emitting Diodes. *ECS J. Solid State Sci. Technol.* 10, 045005 (2021).

58. Shatalov, M. *et al.* High power AlGaN ultraviolet light emitters. *Semicond. Sci. Technol.* 29, 084007 (2014).

59. Park, J.-S., Kim, J. K., Cho, J. & Seong, T.-Y. Review—Group III-Nitride-Based Ultraviolet Light-Emitting Diodes: Ways of Increasing External Quantum Efficiency. *ECS J. Solid State Sci. Technol.* 6, Q42 (2017).

60. Mehnke, F. *et al.* Electrical and optical characteristics of highly transparent MOVPE-grown AlGaN-based tunnel heterojunction LEDs emitting at 232 nm. *Photon. Res., PRJ* 9, 1117–1123 (2021).

61. Yun, J. & Hirayama, H. Investigation of Light-Extraction Efficiency of Flip-Chip AlGaN-Based Deep-Ultraviolet Light-Emitting Diodes Adopting AlGaN Metasurface. *IEEE Photonics Journal* 13, 1–13 (2021).

62. Nicholls, J. *et al.* High performance and high yield sub-240 nm AlN:GaN short period superlattice LEDs grown by MBE on 6 in. sapphire substrates. *Applied Physics Letters* 123, 051105 (2023).

63. Rass, J. *et al.* Enhanced light extraction efficiency of far-ultraviolet-C LEDs by micro-LED array design. *Applied Physics Letters* 122, 263508 (2023).

64. Wang, S. *et al*. Ultrahigh Degree of Optical Polarization above 80% in AlGaN-Based Deep-Ultraviolet LED with Moth-Eye Microstructure. *ACS Photonics* 5, 3534–3540 (2018).

65. Inoue, S., Tamari, N. & Taniguchi, M. 150 mW deep-ultraviolet light-emitting diodes with large-area AlN nanophotonic light-extraction structure emitting at 265 nm. *Applied Physics Letters* 110, 141106 (2017).

66. Wei, J. *et al*. Polarization doping technology towards high performance GaN-based heterostructure devices. *IOP Conf. Ser.: Mater. Sci. Eng.* 479, 012052 (2019).

67. Laleyan, D. A. *et al*. AlN/h-BN Heterostructures for Mg Dopant-Free Deep Ultraviolet Photonics. *Nano Lett.* 17, 3738–3743 (2017).

68. Hirayama, H., Tsukada, Y., Maeda, T. & Kamata, N. Marked Enhancement in the Efficiency of Deep-Ultraviolet AlGaN Light-Emitting Diodes by Using a Multiquantum-Barrier Electron Blocking Layer. *Appl. Phys. Express* 3, 031002 (2010).

69. Wang, Y. *et al*. Deep Ultraviolet Light Source from Ultrathin GaN/AlN MQW Structures with Output Power Over 2 Watt. *Advanced Optical Materials* 7, 1801763 (2019).

70. Kioupakis, E., Rinke, P., Delaney, K. T. & Van de Walle, C. G. Indirect Auger recombination as a cause of efficiency droop in nitride light-emitting diodes. *Applied Physics Letters* 98, 161107 (2011).

71. Römer, F. & Witzigmann, B. Effect of Auger recombination and leakage on the droop in InGaN/GaN quantum well LEDs. *Opt. Express, OE* 22, A1440–A1452 (2014).

72. Bae, W. K. *et al*. Controlling the influence of Auger recombination on the performance of quantum-dot light-emitting diodes. *Nat Commun* 4, 2661 (2013).

73. Rudinsky, M. E. & Karpov, S. Yu. Radiative and Auger Recombination Constants and Internal Quantum Efficiency of (0001) AlGaN Deep-UV Light-Emitting Diode Structures. *physica status solidi (a)* 217, 1900878 (2020).

74. Sulmoni, L. *et al*. Electrical properties and microstructure formation of V/Al-based n-contacts on high Al mole fraction n-AlGaN layers. *Photon. Res., PRJ* 8, 1381–1387 (2020).

75. Letson, B. C. *et al*. Review—Reliability and Degradation Mechanisms of Deep UV AlGaN LEDs. *ECS J. Solid State Sci. Technol.* 12, 066002 (2023).

76. Zollner, C. J., DenBaars, S. P., Speck, J. S. & Nakamura, S. Germicidal ultraviolet LEDs: a review of applications and semiconductor technologies. *Semicond. Sci. Technol.* 36, 123001 (2021).

77. Saifaddin, B. K. *et al*. Fabrication technology for high light-extraction ultraviolet thin-film flip-chip (UV TFFC) LEDs grown on SiC. *Semicond. Sci. Technol.* 34, 035007 (2019).

78. Ooi, Y. K. & Zhang, J. Light Extraction Efficiency Analysis of Flip-Chip Ultraviolet Light-Emitting Diodes With Patterned Sapphire Substrate. *IEEE Photonics Journal* 10, 1–13 (2018).

79. Saifaddin, B. K. *et al*. Impact of roughening density on the light extraction efficiency of thin-film flip-chip ultraviolet LEDs grown on SiC. *Opt. Express, OE* 27, A1074–A1083 (2019).

80. Wu, B. J. *et al*. Growth and characterization of II–VI blue light-emitting diodes using short period superlattices. *Applied Physics Letters* 68, 379–381 (1996).

81. Lundin, W. V. *et al*. Single quantum well deep-green LEDs with buried InGaN/GaN short-period superlattice. *Journal of Crystal Growth* 315, 267–271 (2011).

82. Nikishin, S. A. *et al*. Deep Ultraviolet Light Emitting Diodes Based on Short Period Superlattices of AlN/AlGa(In)N. *Jpn. J. Appl. Phys.* 42, L1362 (2003).

83. Allerman, A. A., Crawford, M. H., Miller, M. A. & Lee, S. R. Growth and characterization of Mg-doped AlGaN–AlN short-period superlattices for deep-UV optoelectronic devices. *Journal of Crystal Growth* 312, 756–761 (2010).

84. Nikishin, S. A. III-Nitride Short Period Superlattices for Deep UV Light Emitters. *Applied Sciences* 8, 2362 (2018).

85. Saxler, A., Mitchel, W. C., Kung, P. & Razeghi, M. Aluminum gallium nitride short-period superlattices doped with magnesium. *Applied Physics Letters* 74, 2023–2025 (1999).

86. Muhin, A. *et al*. Vertical conductivity and Poole–Frenkel-ionization of Mg acceptors in AlGaN short-period superlattices with high Al mole fraction. *Applied Physics Letters* 117, 252101 (2020).

87. Anderson, L. Beyond the limits of AlGaN: High performance sub-240 nm UVC LEDs using SPSL technology. (2023).

88. Monemar, B., Ohlsson, B. J., Gardner, N. F. & Samuelson, L. Chapter Seven - Nanowire-Based Visible Light Emitters, Present Status and Outlook. in *Semiconductors and Semimetals* (eds. Dayeh, S. A., Fontcuberta i Morral, A. & Jagadish, C.) vol. 94 227–271 (Elsevier, 2016).

89. Zhang, Z. *et al*. A 271.8 nm deep-ultraviolet laser diode for room temperature operation. *Appl. Phys. Express* 12, 124003 (2019).

90. Ünlü, M. S. & Strite, S. Resonant cavity enhanced photonic devices. *Journal of Applied Physics* 78, 607–639 (1995).

91. Jennings, D. A. & Varga, A. J. Efficient Second Harmonic Generation in ADP with Two New Fluorescein Dye Lasers. *Journal of Applied Physics* 42, 5171–5172 (1971).

92. Chuangtian, C., Bochang, W., Aidong, J. & Guiming, Y. A NEW-TYPE ULTRAVIOLET SHG CRYSTAL——β-BaB2O4. *Science in China Series B-Chemistry, Biological, Agricultural, Medical & Earth Sciences* (1985).

93. Miyazaki, K., Sakai, H. & Sato, T. Efficient deep-ultraviolet generation by frequency doubling in β-BaB_2O_4 crystals. *Opt. Lett., OL* 11, 797–799 (1986).

94. Luo, Q., Ma, J., Wang, M., Lu, T. & Zhu, X. All-solid-state far-UVC pulse laser at 222 nm wavelength for UVC disinfection. *Chin. Opt. Lett.* 21, 011401 (2023).

95. Zhao, Z. B. *et al.* Inactivation Effect of All-Solid-State 228 nm Far-UVC Pulsed Laser. *Chinese Journal of Lasers-Zhongguo Jiguang* (2022).

96. Ruhnke, N. *et al.* Single-pass UV generation at 2225 nm based on high-power GaN external cavity diode laser. *Opt. Lett.* 40, 2127 (2015).

97. Ulsig, E. Z. & Volet, N. Design study of efficient far-UVC second-harmonic generation using an integrated approach. in *Nonlinear Optics and Applications XII* (eds. Zayats, A. V., Bertolotti, M. & Zheltikov, A. M.) 22 (SPIE, Online Only, Czech Republic, 2021). doi:10.1117/12.2592408.

98. Liu, X. *et al.* Ultra-high-Q UV microring resonators based on a single-crystalline AlN platform. *Optica* 5, 1279 (2018).

99. Alden, D. *et al.* Quasi-phase-matched second harmonic generation of UV light using AlN waveguides. *Applied Physics Letters* 114, 103504 (2019).

100. Pernice, W. H. P., Xiong, C., Schuck, C. & Tang, H. X. Second harmonic generation in phase matched aluminum nitride waveguides and micro-ring resonators. *Applied Physics Letters* 100, 223501 (2012).

101. Guo, X., Zou, C.-L. & Tang, H. X. Second-harmonic generation in aluminum nitride microrings with 2500%/W conversion efficiency. *Optica, OPTICA* 3, 1126–1131 (2016).

102. Ruhnke, N. *et al.* Compact Deep UV System at 222.5 nm Based on Frequency Doubling of GaN Laser Diode Emission. *IEEE Photon. Technol. Lett.* 30, 289–292 (2018).

103. Stanton, E. J. *et al.* Continuous-wave second-harmonic generation in the far-UVC pumped by a blue laser diode. Preprint at http://arxiv.org/abs/2309.04554 (2023).

104. Rodriguez, A., Soljac̆ic, M., Joannopoulos, J. D. & Johnson, S. G. $\chi(2)$ and $\chi(3)$ harmonic generation at a critical power in inhomogeneous doubly resonant cavities. (2007).

105. Bi, Z.-F. *et al.* High-efficiency second-harmonic generation in doubly-resonant χ^(2) microring resonators. *Opt. Express* 20, 7526 (2012).

106. Oto, T., Banal, R. G., Kataoka, K., Funato, M. & Kawakami, Y. 100 mW deep-ultraviolet emission from aluminium-nitride-based quantum wells pumped by an electron beam. *Nature Photon* 4, 767–770 (2010).

107. Harikumar, A. *et al.* Internal quantum efficiency of AlGaN/AlN quantum dot superlattices for electron-pumped ultraviolet sources. *Nanotechnology* 31, 505205 (2020).

108. Chaudhari, A. *et al.* Zinc oxide family semiconductors for ultraviolet radiation emission – A cathodoluminescence study. *Materials Research Bulletin* 153, 111906 (2022).

109. Chaudhari, A., Frederiksen, L. & Vispute, R. D. A light emitting device. (2022).

110. Coe-Sullivan, S., Stevenson, M. & LALEYAN, D. A. Ultraviolet cathodoluminescent lamp, system and method. (2023).

111. Laszczyk, K. & Krysztof, M. Electron beam source for the miniaturized electron microscope on-chip. *Vacuum* 189, 110236 (2021).

112. Kalmykova, Y., Patrício, J., Rosado, L. & Berg, P. E. Out with the old, out with the new – The effect of transitions in TVs and monitors technology on consumption and WEEE generation in Sweden 1996–2014. *Waste Management* 46, 511–522 (2015).

113. Nykänen, H. *et al.* Low energy electron beam induced damage on InGaN/GaN quantum well structure. *Journal of Applied Physics* 109, 083105 (2011).

114. Kioupakis, E. *et al.* Theoretical characterization and computational discovery of ultra-wide-band-gap semiconductors with predictive atomistic calculations. *Journal of Materials Research* 36, 4616–4637 (2021).

115. Yuan, L.-D., Deng, H.-X., Li, S.-S., Wei, S.-H. & Luo, J.-W. Unified theory of direct or indirect band-gap nature of conventional semiconductors. *Phys. Rev. B* 98, 245203 (2018).

116. Goyal, A. *et al.* On the Dopability of Semiconductors and Governing Material Properties. *Chem. Mater.* 32, 4467–4480 (2020).

117. Hill, R. Energy-gap variations in semiconductor alloys. *J. Phys. C: Solid State Phys.* 7, 521 (1974).

118. Zhu, Y. F., Lang, X. Y. & Jiang, Q. The Effect of Alloying on the Bandgap Energy of Nanoscaled Semiconductor Alloys. *Advanced Functional Materials* 18, 1422–1429 (2008).

119. Alferov, Zh. I. The history and future of semiconductor heterostructures. *Semiconductors* 32, 1–14 (1998).

120. Boron nitride. *Wikipedia* (2023).

121. Monteiro, S. N., Skury, A. L. D., de Azevedo, M. G. & Bobrovnitchii, G. S. Cubic boron nitride competing with diamond as a superhard engineering material – an overview. *Journal of Materials Research and Technology* 2, 68–74 (2013).

122. Li, Q. *et al.* Direct Growth of 5 in. Uniform Hexagonal Boron Nitride on Glass for High-Performance Deep-Ultraviolet Light-Emitting Diodes. *Advanced Materials Interfaces* 5, 1800662 (2018).

123. Liu, H. *et al.* Synthesis of hexagonal boron nitrides by chemical vapor deposition and their use as single photon emitters. *Nano Materials Science* 3, 291–312 (2021).

124. Maity, A., Grenadier, S. J., Li, J., Lin, J. Y. & Jiang, H. X. Hexagonal boron nitride: Epitaxial growth and device applications. *Progress in Quantum Electronics* 76, 100302 (2021).

125. Watanabe, K., Taniguchi, T. & Kanda, H. Direct-bandgap properties and evidence for ultraviolet lasing of hexagonal boron nitride single crystal. *Nature Mater* 3, 404–409 (2004).

126. Kubota, Y., Watanabe, K., Tsuda, O. & Taniguchi, T. Deep Ultraviolet Light-Emitting Hexagonal Boron Nitride Synthesized at Atmospheric Pressure. *Science* 317, 932–934 (2007).

127. Evans, D. A. *et al*. Determination of the optical band-gap energy of cubic and hexagonal boron nitride using luminescence excitation spectroscopy. *J. Phys.: Condens. Matter* 20, 075233 (2008).

128. Watanabe, K. & Taniguchi, T. Jahn-Teller effect on exciton states in hexagonal boron nitride single crystal. *Phys. Rev. B* 79, 193104 (2009).

129. Cassabois, G., Valvin, P. & Gil, B. Hexagonal boron nitride is an indirect bandgap semiconductor. *Nature Photon* 10, 262–266 (2016).

130. Laleyan, D. A. *et al*. Epitaxial hexagonal boron nitride with high quantum efficiency. *APL Materials* 11, 051103 (2023).

131. Wu, Q. *et al*. Growth mechanism of AlN on hexagonal BN/sapphire substrate by metal–organic chemical vapor deposition. *CrystEngComm* 19, 5849–5856 (2017).

132. Wu, Q. *et al*. Exfoliation of AlN film using two-dimensional multilayer hexagonal BN for deep-ultraviolet light-emitting diodes. *Appl. Phys. Express* 12, 015505 (2018).

133. Watanabe, K., Taniguchi, T., Niiyama, T., Miya, K. & Taniguchi, M. Far-ultraviolet plane-emission handheld device based on hexagonal boron nitride. *Nature Photon* 3, 591–594 (2009).

134. Mballo, A. *et al*. Towards P-Type Conduction in Hexagonal Boron Nitride: Doping Study and Electrical Measurements Analysis of hBN/AlGaN Heterojunctions. *Nanomaterials* 11, 211 (2021).

135. Lu, S. *et al*. Towards n-type conductivity in hexagonal boron nitride. *Nat Commun* 13, 3109 (2022).

136. Taniguchi, T. *et al*. High pressure synthesis of UV-light emitting cubic boron nitride single crystals. *Diamond and Related Materials* 12, 1098–1102 (2003).

137. Mishima, O., Era, K., Tanaka, J. & Yamaoka, S. Ultraviolet light-emitting diode of a cubic boron nitride *p n* junction made at high pressure. *Applied Physics Letters* 53, 962–964 (1988).

138. Perovskite (structure). *Wikipedia* (2023).

139. Bhalla, A. S., Guo, R. & Roy, R. The perovskite structure—a review of its role in ceramic science and technology. *Materials Research Innovations* 4, 3–26 (2000).

140. Kaur, P. & Singh, K. Review of perovskite-structure related cathode materials for solid oxide fuel cells. *Ceramics International* 46, 5521–5535 (2020).

141. Kim, E.-B., Akhtar, M. S., Shin, H.-S., Ameen, S. & Nazeeruddin, M. K. A review on two-dimensional (2D) and 2D-3D multidimensional perovskite solar cells: Perovskites structures, stability, and photovoltaic performances. *Journal of Photochemistry and Photobiology C: Photochemistry Reviews* 48, 100405 (2021).

142. Lou, J., Feng, J., Liu, S. (Frank) & Qin, Y. Semitransparent Perovskite Solar Cells for Photovoltaic Application. *Solar RRL* 7, 2200708 (2023).

143. Veldhuis, S. A. *et al*. Perovskite Materials for Light-Emitting Diodes and Lasers. *Advanced Materials* 28, 6804–6834 (2016).

144. Yang, X. *et al*. Focus on perovskite emitters in blue light-emitting diodes. *Light Sci Appl* 12, 177 (2023).

145. Chae, S. *et al*. Toward the predictive discovery of ambipolarly dopable ultra-wide-band-gap semiconductors: The case of rutile GeO2. *Applied Physics Letters* 118, 260501 (2021).

146. Lyons, J. L. & Janotti, A. A p-type dopable ultrawide-bandgap oxide. *J. Phys.: Condens. Matter* 36, 085501 (2023).

8. Appendix

8.1. Forecasting results tables

Supplementary Table 1: *Mean years with standard deviation (SD) of cathodoluminescent device forecasts.*

Target	Milestone	Earliest plausible year	SD	Most likely year	SD	Latest plausible year	SD
Lifetime of at least...	1k h	2023.5	1.0	2024.3	1.3	2026.4	2.5
	10k h	2025.8	2.2	2028.4	3.0	2035.8	12.9
	25k h	2029.6	3.7	2036.7	12.7	2042.3	12.5
Wall-plug efficiency of at least...	1%	2024.2	0.8	2025.8	1.9	2030.5	6.0
	3%	2026.9	1.9	2030.3	3.9	2038.3	13.1
	10%	2030.2	2.7	2040.5	12.9	2048.6	14.6
Cost per milliwatt of at most...	$10	2024.1	1.1	2025.3	1.2	2030.8	6.1
	$1	2026.7	1.8	2029.4	2.8	2038.3	13.0
	$0.10	2029.6	2.1	2039.2	13.1	2047.4	14.8

Supplementary Table 2: *Mean years with standard deviation (SD) of second-harmonic generation device forecasts.*

Target	Milestone	Earliest plausible year	SD	Most likely year	SD	Latest plausible year	SD
Lifetime of at least…	1k h	2023.7	0.9	2024.3	1.1	2026.9	3.5
	10k h	2024.8	2.0	2026.1	2.6	2030.0	6.3
	25k h	2026.3	2.9	2028.9	4.4	2034.2	9.7
Wall-plug efficiency of at least…	1%	2023.5	0.8	2024.6	0.7	2026.3	1.8
	3%	2024.5	1.6	2026.3	1.8	2028.9	3.2
	10%	2027.5	3.2	2030.8	4.6	2035.9	6.3
Cost per milliwatt of at most…	$10	2023.7	1.0	2024.5	0.5	2033.7	17.8
	$1	2025.0	1.4	2026.7	1.4	2036.0	16.7
	$0.10	2026.3	2.2	2031.0	4.9	2039.8	14.8

Supplementary Table 3: *Mean years with standard deviation (SD) of electroluminescent device forecasts.*

Target	Milestone	Earliest plausible year	SD	Most likely year	SD	Latest plausible year	SD
Lifetime of at least...	1k h	2023.8	1.2	2024.9	1.7	2027.5	3.0
	10k h	2025.9	1.8	2028.0	2.3	2031.8	5.2
	25k h	2028.8	3.4	2032.5	6.1	2038.5	9.6
Wall-plug efficiency of at least...	1%	2024.0	0.6	2025.2	1.4	2027.4	2.7
	3%	2025.9	1.0	2028.1	1.4	2031.8	4.8
	10%	2029.7	2.4	2032.7	3.6	2039.3	9.0
Cost per milliwatt of at most...	$10	2024.6	1.8	2025.6	2.2	2028.1	3.0
	$1	2027.4	1.8	2029.4	2.4	2035.3	7.5
	$0.10	2031.6	4.0	2034.1	4.1	2042.1	8.4

8.2. Forecasting results by target metric

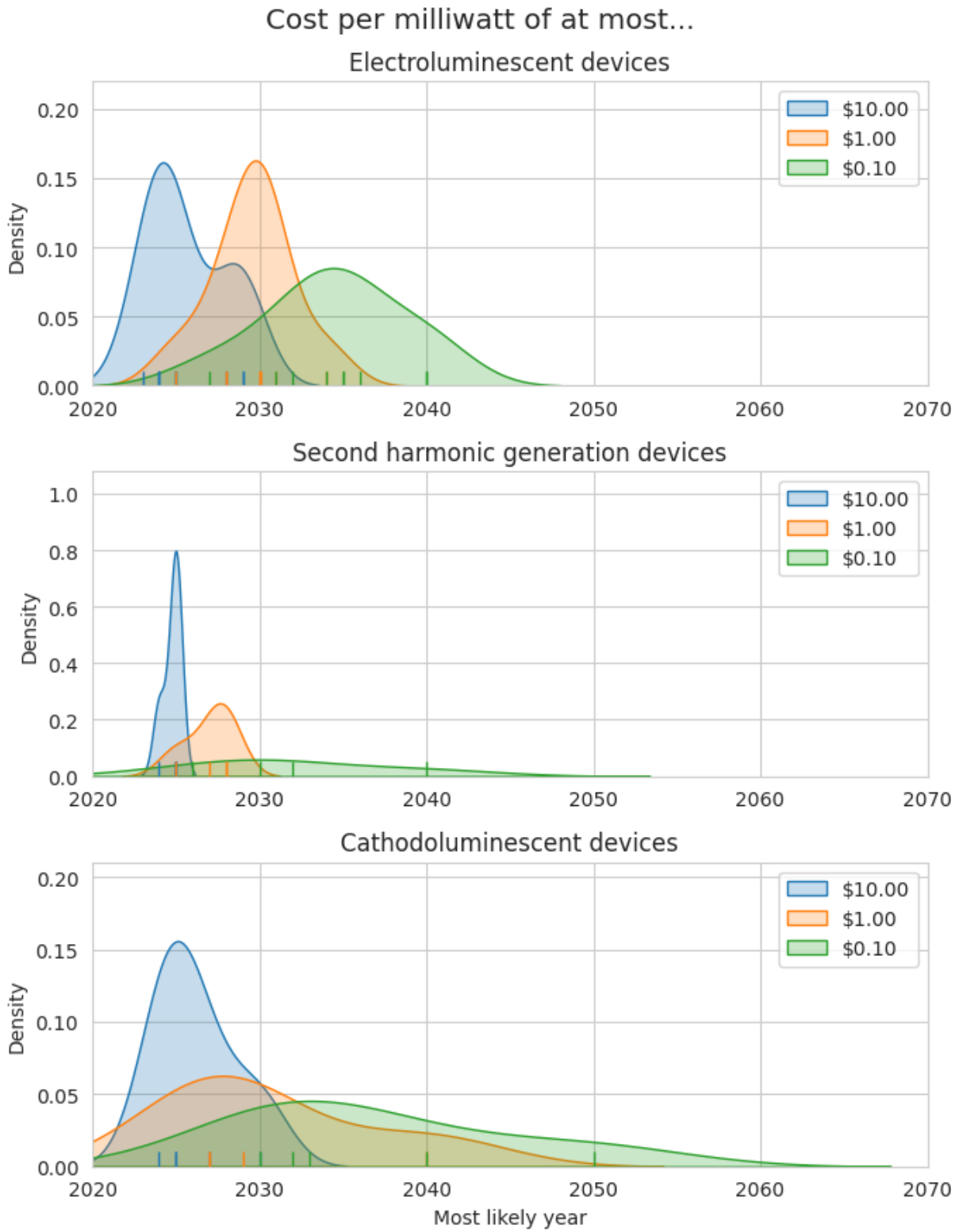

Supplementary Figure 1: *KDE plots of cost-per-milliwatt forecasts of all three approaches.*

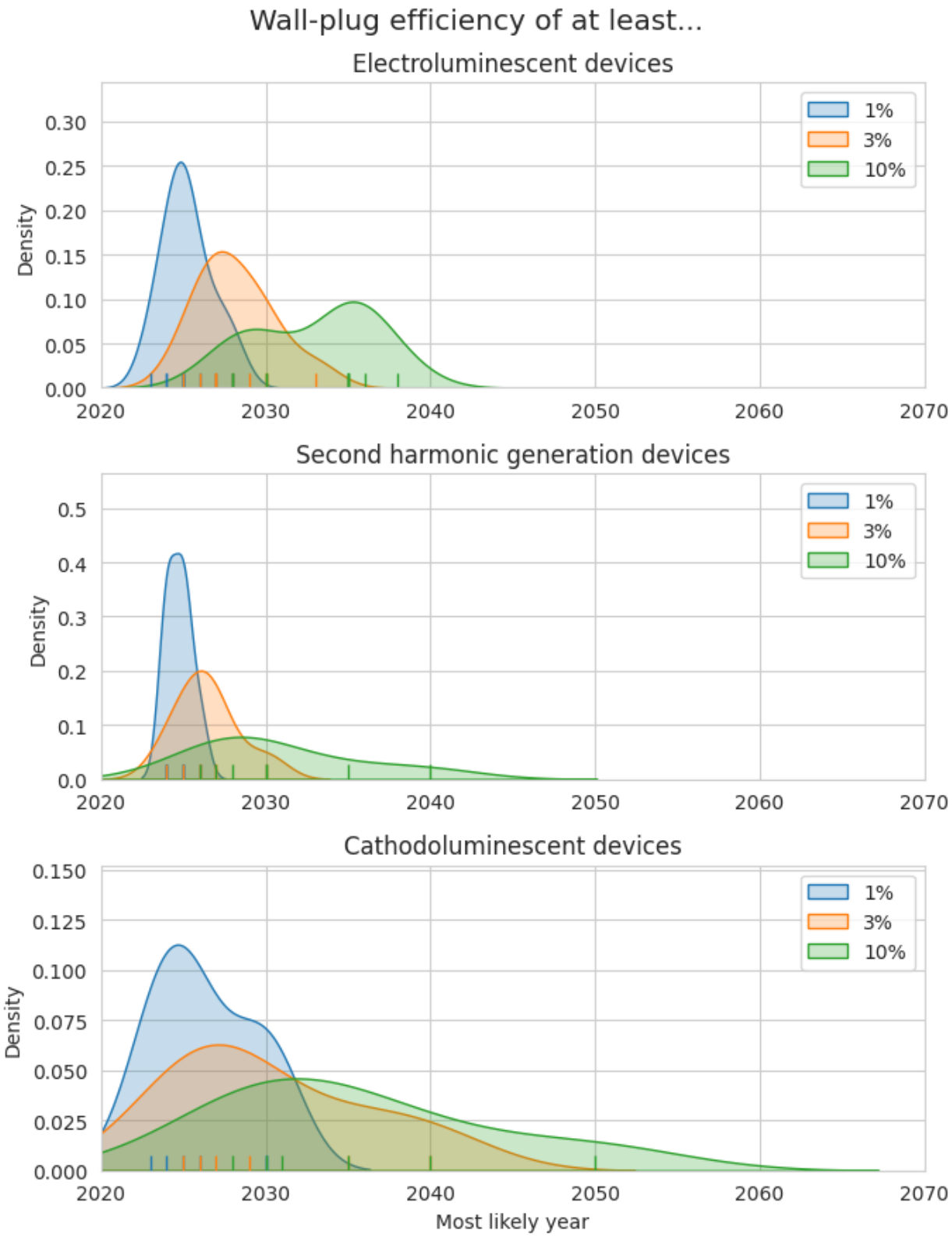

Supplementary Figure 2: *KDE plots of wall-plug efficiency forecasts of all three approaches.*

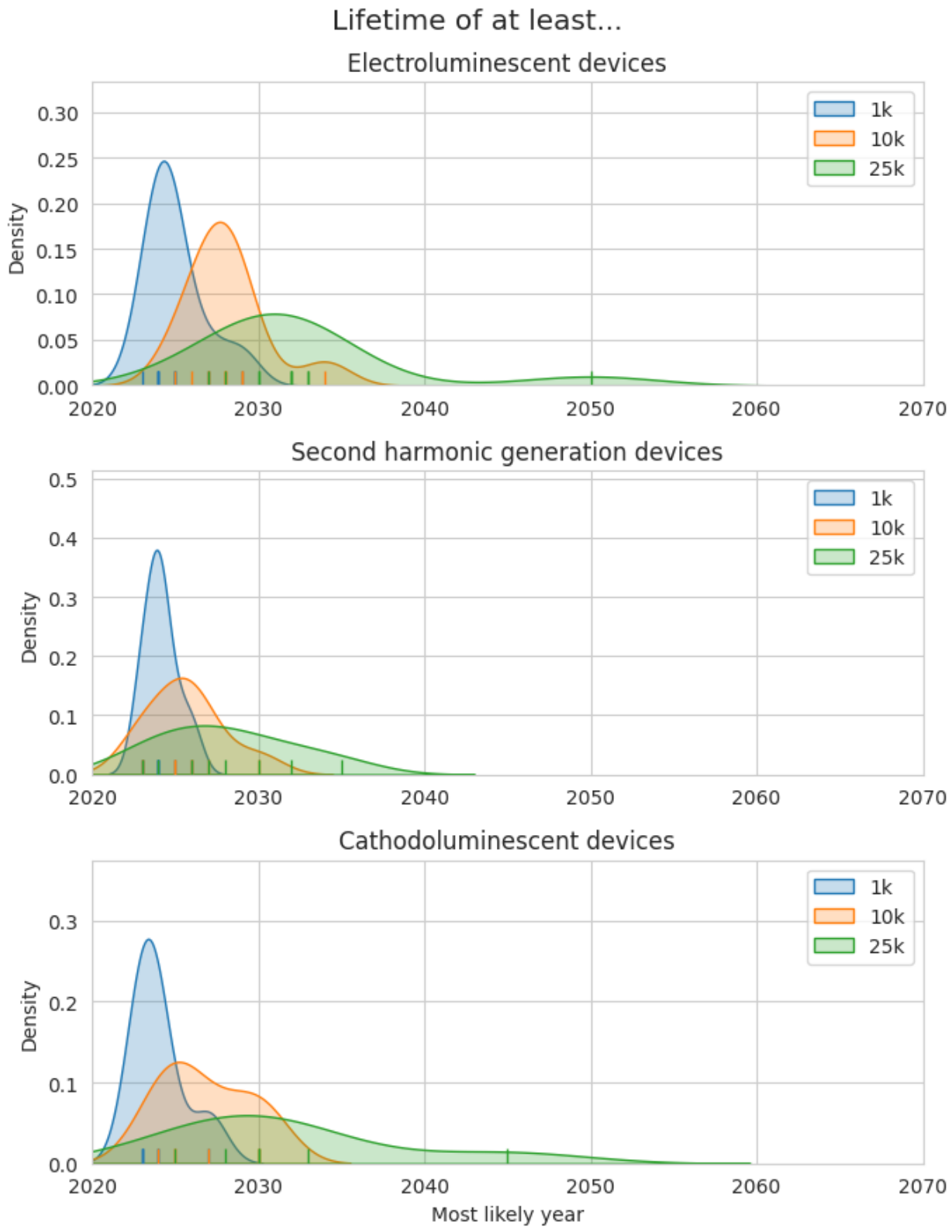

Supplementary Figure 3: *KDE plots of lifetime forecasts of all three approaches.*